Ex Vivo Expansion of EPC by TPO

A Peripheral Blood

B Peripheral Blood   Cord Blood

CD31 FITC

C Peripheral Blood

D a   **b**

Treatment

c

Treatment

CD31 FITC

FIGURE 4. **Stimulative effects of TPO on induction of CD31^{bright} cells.** A, alteration of the cell number of cultivated AC133$^+$ cells for 1 week in the combination of growth factors. Mix, VEGF + SCF + TPO. B, the flow cytometric histogram of AC133$^+$-derived cells stained with FITC-labeled anti-CD31 antibody after a 1-week culture. The representing number in the flow cytometric histogram indicates the percentage of the CD31^{bright} cell population. The left panels are peripheral blood, and the right panels are cord blood. C, CD31^{bright}
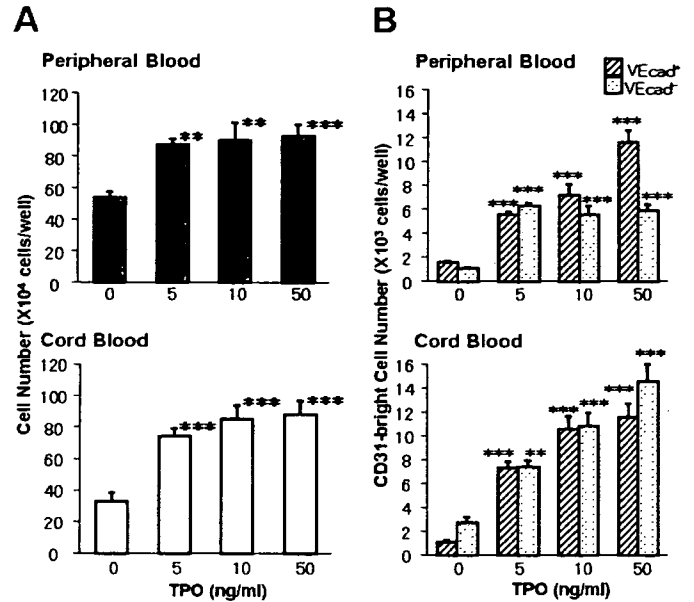
A Peripheral Blood

Cord Blood

B Peripheral Blood

Cord Blood

FIGURE 5. **Dose-dependent effects of TPO on the induction of CD31^{bright} cells from AC133$^+$ cells.** AC133$^+$ cells were treated with various concentrations of TPO for 1 week. The left panels (A) are the total cell number of cultured AC133$^+$ cells from peripheral blood (upper panel) and cord blood (lower panel). The right panels (B) are the calculated CD31^{bright} cell number from peripheral blood (upper panel) and cord blood (lower panel). Columns and bars represent the means ± S.D. (**, p < 0.01; ***, p < 0.001). Striped and dotted columns represent CD31^{bright}VEcad$^+$ cells and CD31^{bright}VEcad$^-$ cells, respectively.

number of CD31^{bright} cells when compared with the control (Fig. 4D, panel c). The concomitant treatment with both VEGF and TPO showed a synergic increase in the number of CD31^{bright} cells (Fig. 4D, panel c).

When AC133$^+$ cells were cultured with various concentrations of TPO in the presence of constant concentrations of VEGF (50 ng/ml), the total cell number from both peripheral blood (Fig. 5A, upper panel) and cord blood (Fig. 5A, lower panel) significantly increased at 5 ng/ml of TPO when compared with the control, and there was no significant difference in the total cell number from 5 to 50 ng/ml of TPO. However, TPO increased the ratio of CD31^{bright} cells of flow cytometry dose-dependently as follows: control, 0.50%; 5 ng/ml, 1.36%; 10 ng, 1.42%; 50 ng/ml 1.90% in peripheral blood and control, 1.16%; 5 ng/ml, 1.99%; 10 ng, 2.51%; 50 ng/ml 2.96% in cord blood. TPO markedly induced the differentiation of AC133$^+$ cells into CD31^{bright}VEcad$^+$ cells in the case of both peripheral blood (Fig. 5B, upper panel) and cord blood (Fig. 5B, lower panel) in a dose-dependent manner. In the case of cord blood cells, differentiation into CD31^{bright}VEcad$^-$ cells was also induced by TPO.

The effects of TPO on total cell number during 6-day culture of AC133$^+$ cells were determined. Although the total cell num-

cells numbers were calculated by both the total cell number and the ratio of the CD31^{bright} population. D, the effects of TPO alone on EPC differentiation derived from AC133$^+$ cells of cord blood. The upper left panel (a) shows the total cell number after a 1-week culture, the right panels (b) show the flow cytometric histogram of AC133$^+$-derived cells stained with FITC-labeled anti-CD31 antibody, and the lower left panel (c) shows the calculated CD31^{bright} cell number. Columns and bars represent the means ± S.D. (*, p < 0.05; **, p < 0.01; ***, p < 0.001). NS, not significant; Cont, control.

NOVEMBER 16, 2007·VOLUME 282·NUMBER 46

JOURNAL OF BIOLOGICAL CHEMISTRY **33511**

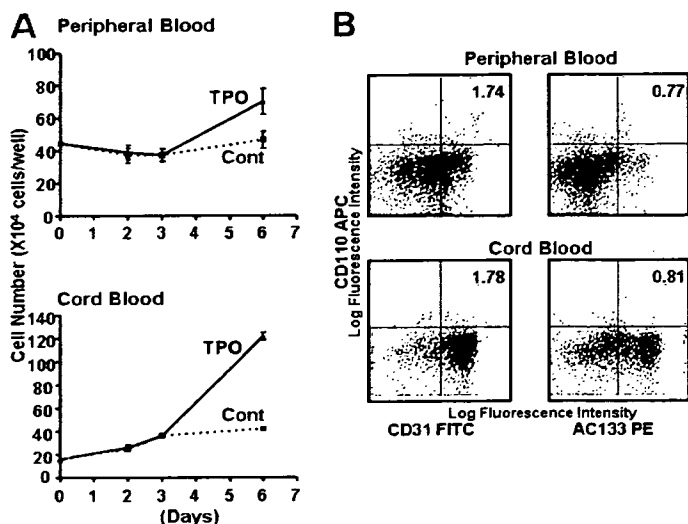**A** Peripheral Blood

B

Peripheral Blood

Cord Blood

FIGURE 6. **Time-course analysis of TPO-treated AC133⁺ cells and expression of TPO receptor (CD110).** *A*, alteration of cell number was counted at 2, 3, and 6 days. Solid and dotted lines indicate TPO-treated cells and control ((Cont) VEGF alone) cells, respectively. The results represent mean ± S.E. of triplicate wells. *B*, flow cytometric analysis of CD110 expression on AC133⁺ cells cultured for 3 days was carried out. The *y* axis represents the log fluorescence intensity of CD110-allophycocyanin (APC), and the *x* axis represents that of CD31-FITC (left panels) and AC133-PE (right panels). The number in the flow cytometric dot blot indicates the percentage of CD110⁺ CD31⁺ and CD110⁺ AC133⁺ populations, respectively. The upper panels are peripheral blood, and the lower panels are cord blood.

ber from AC133⁺ cells slightly and constantly increased from day 0 to day 6 in the absence of TPO, total cells markedly increased after the third day in the presence of TPO (Fig. 6A). Next, the alternation of TPO receptor (CD110) expression was analyzed during the cultivation of AC133⁺ cells. Although the percentages of both AC133⁺ CD110⁺ cells and CD31⁺ CD110⁺ cells were 0% just after magnetic cell sorting, 3 days after the cultivation, ~2% of CD31⁺ CD110⁺ cells (Fig. 6B, left panel) and 1% of AC133⁺ CD110⁺ cells (Fig. 6B, right panel) appeared from AC133⁺ cells in the peripheral blood and cord blood, respectively. These data indicate the possibility that sorted AC133⁺ cells may differentiate into AC133⁺ CD110⁺ cells and may subsequently proliferate and differentiate into EPCs in response to TPO.

It has been reported that TPO activates the PI3K/Akt pathway (28) or JAK/STAT pathway (20, 29, 30) in target cells. In addition, in the present study, TPO induced a marked proliferation of AC133⁺ cells after 3-day culture, and CD110 expression in cells cultured for 3 days from both cord blood and peripheral blood was also observed (Fig. 6, A and B). We then attempted to determine whether TPO activates Akt or STAT in AC133⁺ cells cultured for 3 days by analyzing the phosphorylation at Ser-473 of Akt or the phosphorylation at Tyr-705 of STAT3, which are the active forms of Akt or STAT3, respectively. As shown in Fig. 7A, phosphorylation at Ser-473 of Akt was stimulated by both VEGF and TPO at 15 min and was more markedly stimulated by concomitant treatment with VEGF and TPO than by a single treatment (Fig. 7A, top panel). Phosphorylation at Tyr-705 of STAT3 was observed only in the presence of TPO, and unlike in the phosphorylation at Ser-473 of Akt, an increased amount of phosphorylation was not observed in the concomitant presence of VEGF and TPO (Fig. 7A, third panel).
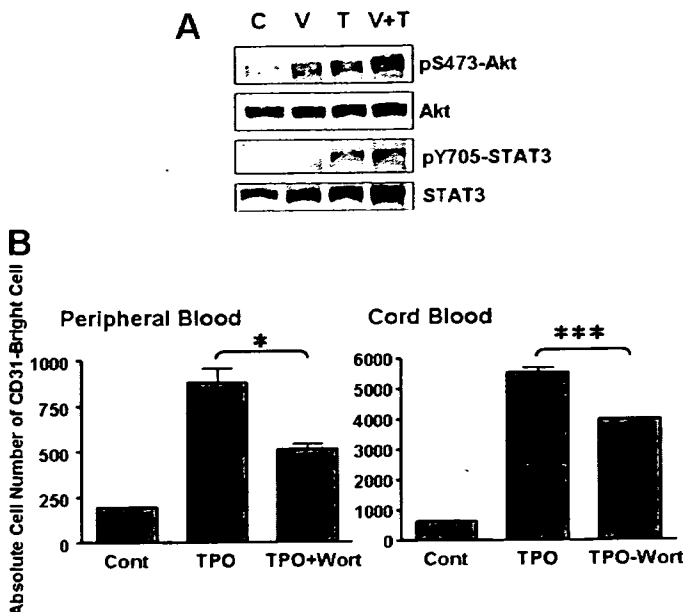
A

C   V   T   V+T

pS473-Akt

Akt

pY705-STAT3

STAT3

B

Peripheral Blood   Cord Blood

FIGURE 7. **Analysis of TPO-induced signal transduction on AC133⁺ cells of cord blood.** *A*, activation of Akt or STAT3 was analyzed by Western blotting with anti-phospho-specific Ser-473-Akt antibody (top panel) and reprobed with anti-Akt antibody (second panel), or with anti-phospho-specific Tyr-705-STAT3 antibody (third panel) and reprobed with anti-STAT3 antibody (lower panel) after stimulation by VEGF, TPO, or both VEGF and TPO for 15 min using 3-day-cultured AC133⁺ cells. *C*, control; *V*, VEGF; *T*, TPO. *B*, the effects of wortmannin on CD31^bright cell induction were investigated. The right panel shows peripheral blood, and the left panel shows cord blood. The *y* axis represents the CD31^bright cell number. Wort, 100 nM wortmannin. Columns and bars represent the means ± S.E. (*, p < 0.05; ***, p < 0.001). Cont, control.

On the other hand, there was no difference in the expression of Akt and STAT3 protein levels (Fig. 7A, second panel and bottom panel, respectively). The induction of CD31^bright cells was not perfectly but significantly inhibited by wortmannin, an inhibitor of PI3K, suggesting that the PI3K/Akt pathway plays an important role in TPO-induced EPC differentiation (Fig. 7B).

DISCUSSION

We have previously reported that CD31^bright cells derived from AC133⁺ cells in human peripheral blood are EPCs (25). In the present study, CD31^bright cells also appeared from AC133⁺ cells prepared from cord blood, which are a rich source of stem cells during the early period of cultivation (Fig. 1, A and B). When cells were separated in terms of CD31 expression (Fig. 1C), CD31^bright cells differentiated into KDR-positive and eNOS-positive adherent cells. These data indicate that CD31^bright cells derived from AC133⁺ cells in cord blood have some characteristics similar to those of EPCs in peripheral blood. Although these EPCs in both cord blood and peripheral blood could not form tube-like structure by themselves on Matrigel (data not shown), they secreted angiogenic growth factors (Fig. 2) such as VEGF, IL-8 (31, 32), and monocyte chemoattractant protein-1 (MCP-1) (33). It has been reported that there are at least two types of EPCs: early EPCs and late EPCs. Early EPCs are unable to form tube-like structures and secrete VEGF and IL-8 showing peak growth at 2–3 weeks (9, 26, 27). Late EPCs with the ability to proliferate and having a cobblestone shape appear late at 2–3 weeks, show exponential growth at 4–8 weeks, and have the ability to form tube-like structures

(26, 27, 34). Rehman *et al.* (9) have reported that EPCs derived from monocytes/macrophages do not proliferate but instead release potent proangiogenic growth factors. In many studies (9, 26, 27, 35–37), because the origin of early EPCs was $CD14^+$ cells or was not precluded by monocytic cells, CD14 expression was still observed in the EPCs after cultivation. In our study, in which $AC133^+$ cells were used as the origin of the EPCs, CD14 expression was not observed in $CD31^{bright}$ cells induced by TPO (Fig. 3*B*). Although the $CD31^{bright}$ cells identified as EPCs in this report and in a previous report did not correspond to their cells in terms of the origin of the cells or cell surface markers, these cells may be early EPCs that can release potent proangiogenic growth factors (Fig. 2). In any event, EPCs are thought to be a heterogeneous population, unlike late EPCs, which have a high ability to proliferate.

Circulating EPCs are up-regulated under physiological or pathological conditions and also by 3-hydroxy-3-methyl-glutaryl-CoA reductase inhibitors (14, 15) and cytokines such as erythropoietin (11–13) and G-CSF (10). In this report, we have revealed the possibility of marked expansion of EPCs *in vitro* by TPO. Brizzi *et al.* (20) have reported that TPO directly stimulates endothelial cell motility and neoangiogenesis. In the present study, TPO may have played a stimulatory role in the differentiation of EPCs from circulating stem cells.

Although both TPO and SCF have the same potency with regard to proliferation of $AC133^+$ cells (Fig. 4*A*), TPO specifically induces an increase in the ratio of the $CD31^{bright}$ cell population when compared with SCF (Fig. 4, *B* and *C*). To develop useful cell therapy products for severe ischemia, it has been considered desirable to establish the efficient expansion of EPCs *in vitro*. Thrombopoietin could increase $CD31^{bright}$ cells (EPCs) even in the absence of VEGF. Kirito *et al.* (38) have reported that TPO enhances expression of VEGF in hematopoietic cells through induction of hypoxia-inducible factor 1α. These observations suggest the possibility that the production of EPCs by TPO may be supported by VEGF produced by $AC133^+$ cells. However, from the perspective that TPO and VEGF have synergistic effects on the induction of EPCs, TPO seems to induce EPCs through another signaling cascade.

Thrombopoietin is a major regulator of the proliferation, differentiation, and maturation of megakaryocytes (39, 40). The results from recent studies suggest that TPO can act not only as a lineage-specific hematopoietic growth factor but also can affect other hematopoietic cell types. For example, TPO alone does not induce proliferation of long term repopulating hematopoietic stem cells. However, in combination with SCF or IL-3, TPO has several synergistic effects on cell proliferation (19). Our results have revealed a new role of TPO in the production of EPCs.

In the process of differentiation of $AC133^+$ cells into $CD31^{bright}$ cells, both peripheral blood and cord blood appear to be very similar. $AC133^+$ cells of cord blood, however, have a stronger ability to proliferate than those of peripheral blood (Fig. 6*A*). Moreover, TPO stimulates the induction of $CD31^{bright}VEcad^-$ cells only from cord blood (Fig. 5*B*) at high concentrations. Hur *et al.* (26) have reported that $VEcad^-$ EPCs are thought to be an early EPC. It is therefore thought that $AC133^+$ cells of cord blood are more immature than those of peripheral blood.

Although the total cell number treated with TPO slightly increased in a dose-dependent manner (Fig. 5*A*), the $CD31^{bright}$ cell number markedly increased as the TPO concentration increased (Fig. 5*B*). These data suggest the possibility that a higher concentration of TPO may be needed for $CD31^{bright}$ cell induction from $AC133^+$ cells.

When $AC133^+$ cells were stimulated by TPO or VEGF, an increase in the phosphorylation of Akt at Ser-473 was observed. This increase was strongly enhanced by concomitant treatment with VEGF and TPO (Fig. 7*A*). The induction of $CD31^{bright}$ cells by these growth factors (Fig. 4*D*) was consistent with the increase in the phosphorylation of Akt at Ser-473. TPO but not VEGF could also stimulate the phosphorylation of STAT3 at Tyr-705. We previously reported that the PI3K/p70 S6 kinase pathway and the JAK/STAT3 pathway were important for proliferation and differentiation, respectively, in neutrophilic differentiation (41, 42). Owing to the stimulation of both the PI3K/Akt and the JAK/STAT pathways, we postulated that TPO may be a stronger stimulator of EPC production than VEGF. As shown in Fig. 7*B*, however, wortmannin could not completely inhibit the induction of $CD31^{bright}$ cells. Therefore, a pathway other than the PI3K/Akt pathway may also work for the proliferation and differentiation of EPCs.

The observation of unfavorable angiogenesis has recently been reported after transplantation of bone marrow mononuclear cells in patients with thromboangiitis obliterans (43). Moreover, transfer of both spleen cell-derived EPCs and bone marrow mononuclear cells accelerate atherosclerosis in apoE knockout mice, whereas EPC transfer reduces markers associated with plaque stability (44). These observations suggest that transplantation of differentiated cells from EPCs may be useful therapy as regenerative medicine.

In conclusion, we have demonstrated a new role of TPO in enhancing the differentiation of $AC133^+$ cells into $CD31^{bright}$ cells (EPCs) *in vitro*. These findings may contribute to further development of cell therapy for critical ischemia.

REFERENCES

1. Asahara, T., Masuda, H., Takahashi, T., Kalka, C., Pastore, C., Silver, M., Kearne, M., Magner, M., and Isner, J. M. (1999) *Circ. Res.* 85, 221–228
2. Asahara, T., Murohara, T., Sullivan, A., Silver, M., van der Zee, R., Li, T., Witzenbichler, B., Schatteman, G., and Isner, J. M. (1997) *Science* 275, 964–967
3. Asahara, T., Takahashi, T., Masuda, H., Kalka, C., Chen, D., Iwaguro, H., Inai, Y., Silver, M., and Isner, J. M. (1999) *EMBO J.* 18, 3964–3972
4. Shi, Q., Rafii, S., Wu, M. H., Wijelath, E. S., Yu, C., Ishida, A., Fujita, Y., Kothari, S., Mohle, R., Sauvage, L. R., Moore, M. A., Storb, R. F., and Hammond, W. P. (1998) *Blood* 92, 362–367
5. Takahashi, T., Kalka, C., Masuda, H., Chen, D., Silver, M., Kearney, M., Magner, M., Isner, J. M., and Asahara, T. (1999) *Nat. Med.* 5, 434–438
6. Nieda, M., Nicol, A., Denning-Kendall, P., Sweetenham, J., Bradley, B., and Hows, J. (1997) *Br. J. Haematol.* 98, 775–777
7. Gill, M., Dias, S., Hattori, K., Rivera, M. L., Hicklin, D., Witte, L., Girardi, L., Yurt, R., Himel, H., and Rafii, S. (2001) *Circ. Res.* 88, 167–174
8. Peichev, M., Naiyer, A. J., Pereira, D., Zhu, Z., Lane, W. J., Williams, M.,

Oz, M. C., Hicklin, D. J., Witte, L., Moore, M. A., and Rafii, S. (2000) *Blood* **95**, 952–958

9. Rehman, J., Li, J., Orschell, C. M., and March, K. L. (2003) *Circulation* **107**, 1164–1169

10. Kocher, A. A., Schuster, M. D., Szabolcs, M. J., Takuma, S., Burkhoff, D., Wang, J., Homma, S., Edwards, N. M., and Itescu, S. (2001) *Nat. Med.* **7**, 430–436

11. Bahlmann, F. H., De Groot, K., Spandau, J. M., Landry, A. L., Hertel, B., Duckert, T., Boehm, S. M., Menne, J., Haller, H., and Fliser, D. (2004) *Blood* **103**, 921–926

12. Bahlmann, F. H., DeGroot, K., Duckert, T., Niemczyk, E., Bahlmann, E., Boehm, S. M., Haller, H., and Fliser, D. (2003) *Kidney Int.* **64**, 1648–1652

13. Heeschen, C., Aicher, A., Lehmann, R., Fichtlscherer, S., Vasa, M., Urbich, C., Mildner-Rihm, C., Martin, H., Zeiher, A. M., and Dimmeler, S. (2003) *Blood* **102**, 1340–1346

14. Dimmeler, S., Aicher, A., Vasa, M., Mildner-Rihm, C., Adler, K., Tiemann, M., Rutten, H., Fichtlscherer, S., Martin, H., and Zeiher, A. M. (2001) *J. Clin. Investig.* **108**, 391–397

15. Llevadot, J., Murasawa, S., Kureishi, Y., Uchida, S., Masuda, H., Kawamoto, A., Walsh, K., Isner, J. M., and Asahara, T. (2001) *J. Clin. Investig.* **108**, 399–405

16. Kaushansky, K., Lok, S., Holly, R. D., Broudy, V. C., Lin, N., Bailey, M. C., Forstrom, J. W., Buddle, M. M., Oort, P. J., Hagen, F. S., Roth, G. J., Papayannopoulou, T., and Foster, D. C. (1994) *Nature* **369**, 568–571

17. Fox, N., Priestley, G., Papayannopoulou, T., and Kaushansky, K. (2002) *J. Clin. Investig.* **110**, 389–394

18. Kimura, S., Roberts, A. W., Metcalf, D., and Alexander, W. S. (1998) *Proc. Natl. Acad. Sci. U. S. A.* **95**, 1195–1200

19. Sitnicka, E., Lin, N., Priestley, G. V., Fox, N., Broudy, V. C., Wolf, N. S., and Kaushansky, K. (1996) *Blood* **87**, 4998–5005

20. Brizzi, M. F., Battaglia, E., Montrucchio, G., Dentelli, P., Del Sorbo, L., Garbarino, G., Pegoraro, L., and Camussi, G. (1999) *Circ. Res.* **84**, 785–796

21. Kaushansky, K., Lin, N., Grossmann, A., Humes, J., Sprugel, K. H., and Broudy, V. C. (1996) *Exp. Hematol.* **24**, 265–269

22. Broudy, V. C., Lin, N. L., and Kaushansky, K. (1995) *Blood* **85**, 1719–1726

23. Kaushansky, K., Broudy, V. C., Grossmann, A., Humes, J., Lin, N., Ren, H. P., Bailey, M. C., Papayannopoulou, T., Forstrom, J. W., and Sprugel, K. H. (1995) *J. Clin. Investig.* **96**, 1683–1687

24. Kobayashi, M., Laver, J. H., Kato, T., Miyazaki, H., and Ogawa, M. (1995) *Blood* **86**, 2494–2499

25. Kanayasu-Toyoda, T., Yamaguchi, T., Oshizawa, T., and Hayakawa, T. (2003) *J. Cell. Physiol.* **195**, 119–129

26. Hur, J., Yoon, C. H., Kim, H. S., Choi, J. H., Kang, H. J., Hwang, K. K., Oh, B. H., Lee, M. M., and Park, Y. B. (2004) *Arterioscler. Thromb. Vasc. Biol.* **24**, 288–293

27. Yoon, C. H., Hur, J., Park, K. W., Kim, J. H., Lee, C. S., Oh, I. Y., Kim, T. Y., Cho, H. J., Kang, H. J., Chae, I. H., Yang, H. K., Oh, B. H., Park, Y. B., and Kim, H. S. (2005) *Circulation* **112**, 1618–1627

28. Miyakawa, Y., Rojnuckarin, P., Habib, T., and Kaushansky, K. (2001) *J. Biol. Chem.* **276**, 2494–2502

29. Drachman, J. G., Sabath, D. F., Fox, N. E., and Kaushansky, K. (1997) *Blood* **89**, 483–492

30. Kirito, K., Watanabe, T., Sawada, K., Endo, H., Ozawa, K., and Komatsu, N. (2002) *J. Biol. Chem.* **277**, 8329–8337

31. Li, A., Dubey, S., Varney, M. L., Dave, B. J., and Singh, R. K. (2003) *J. Immunol.* **170**, 3369–3376

32. Mizukami, Y., Jo, W. S., Duerr, E. M., Gala, M., Li, J., Zhang, X., Zimmer, M. A., Iliopoulos, O., Zukerberg, L. R., Kohgo, Y., Lynch, M. P., Rueda, B. R., and Chung, D. C. (2005) *Nat. Med.* **11**, 992–997

33. Salcedo, R., Ponce, M. L., Young, H. A., Wasserman, K., Ward, J. M., Kleinman, H. K., Oppenheim, J. J., and Murphy, W. J. (2000) *Blood* **96**, 34–40

34. Lin, Y., Weisdorf, D. J., Solovey, A., and Hebbel, R. P. (2000) *J. Clin. Investig.* **105**, 71–77

35. Assmus, B., Schachinger, V., Teupe, C., Britten, M., Lehmann, R., Dobert, N., Grunwald, F., Aicher, A., Urbich, C., Martin, H., Hoelzer, D., Dimmeler, S., and Zeiher, A. M. (2002) *Circulation* **106**, 3009–3017

36. Kalka, C., Masuda, H., Takahashi, T., Kalka-Moll, W. M., Silver, M., Kearney, M., Li, T., Isner, J. M., and Asahara, T. (2000) *Proc. Natl. Acad. Sci. U. S. A.* **97**, 3422–3427

37. Kawamoto, A., Gwon, H. C., Iwaguro, H., Yamaguchi, J. I., Uchida, S., Masuda, H., Silver, M., Ma, H., Kearney, M., Isner, J. M., and Asahara, T. (2001) *Circulation* **103**, 634–637

38. Kirito, K., Fox, N., Komatsu, N., and Kaushansky, K. (2005) *Blood* **105**, 4258–4263

39. Kelemen, E., Cserhati, I., and Tanos, B. (1958) *Acta Haematol. (Basel)* **20**, 350–355

40. Yamamoto, S. (1957) *Acta Haematol. Jpn.* **20**, 163

41. Kanayasu-Toyoda, T., Yamaguchi, T., Uchida, E., and Hayakawa, T. (1999) *J. Biol. Chem.* **274**, 25471–25480

42. Yamaguchi, T., Mukasa, T., Uchida, E., Kanayasu-Toyoda, T., and Hayakawa, T. (1999) *J. Biol. Chem.* **274**, 15575–15581

43. Miyamoto, K., Nishigami, K., Nagaya, N., Akutsu, K., Chiku, M., Kamei, M., Soma, T., Miyata, S., Higashi, M., Tanaka, R., Nakatani, T., Nonogi, H., and Takeshita, S. (2006) *Circulation* **114**, 2679–2684

44. George, J., Afek, A., Abashidze, A., Shmilovich, H., Deutsch, V., Kopolovich, J., Miller, H., and Keren, G. (2005) *Arterioscler. Thromb. Vasc. Biol.* **25**, 2636–2641

Granulocyte Colony-Stimulating Factor Promotes the Translocation of Protein Kinase Cι in Neutrophilic Differentiation Cells

TOSHIE KANAYASU-TOYODA,[1] TAKAYOSHI SUZUKI,[1] TADASHI OSHIZAWA,[1] ERIKO UCHIDA,[2] TAKAO HAYAKAWA,[2] AND TERUHIDE YAMAGUCHI[1]*

[1] Division of Cellular and Gene Therapy Products, National Institute of Health Sciences, Tokyo, Japan

[2] National Institute of Health Sciences, Tokyo, Japan

Previously, we suggested that the phosphatidylinositol 3-kinase (PI3K)-p70 S6 kinase (p70 S6K) pathway plays an important role in granulocyte colony-stimulating factor (G-CSF)-dependent enhancement of the neutrophilic differentiation and proliferation of HL-60 cells. While atypical protein kinase C (PKC) has been reported to be a regulator of p70 S6K, abundant expression of PKCι was observed in myeloid and lymphoid cells. Therefore, we analyzed the participation of PKCι in G-CSF-dependent proliferation. The maximum stimulation of PKCι was observed from 15 to 30 min after the addition of G-CSF. From 5 to 15 min into this lag time, PKCι was found to translocate from the nucleus to the membrane. At 30 min it re-translocated to the cytosol. This dynamic translocation of PKCι was also observed in G-CSF-stimulated myeloperoxidase-positive cells differentiated from cord blood cells. Small interfering RNA for PKCι inhibited G-CSF-induced proliferation and the promotion of neutrophilic differentiation of HL-60 cells. These data indicate that the G-CSF-induced dynamic translocation and activation processes of PKCι are important to neutrophilic proliferation.

J. Cell. Physiol. 211: 189–196, 2007. © 2006 Wiley-Liss, Inc.

Hematopoietic cell differentiation is regulated by a complex network of growth and differentiation factors (Tenen et al., 1997; Ward et al., 2000). Granulocyte colony-stimulating factor (G-CSF) and its receptors are pivotal to the differentiation of myeloid precursors into mature granulocytes. In previous studies (Kanayasu-Toyoda et al., 2002) on the neutrophilic differentiation of HL-60 cells treated with either dimethyl sulfoxide (DMSO) or retinoic acid (RA), heterogeneous transferrin receptor (Trf-R) populations—transferrin receptor-positive (Trf-R$^+$) cells and transferrin receptor-negative (Trf-R$^-$) cells—appeared 2 days after the addition of DMSO or RA. The Trf-R$^+$ cells were proliferative-type cells that had higher enzyme activity of phosphatidylinositol 3-kinase (PI3K) and protein 70 S6 kinase (p70 S6K), whereas the Trf-R$^-$ cells were differentiation-type cells of which Tyr705 in STAT3 was much more phosphorylated by G-CSF. Inhibition of either PI3K by wortmannin or p70 S6K by rapamycin was found to eliminate the difference in differentiation and proliferation abilities between Trf-R$^+$ and Trf-R$^-$ cells in the presence of G-CSF (Kanayasu-Toyoda et al., 2002). From these results, we concluded that proteins PI3K and p70 S6K play important roles in the growth of HL-60 cells and negatively regulate neutrophilic differentiation. On the other hand, the maximum kinase activity of PI3K was observed at 5 min after the addition of G-CSF (Kanayasu-Toyoda et al., 2002) and that of p70 S6K was observed between 30 and 60 min after, indicating a lag time between PI3K and p70 S6K activation. It is conceivable that any signal molecule(s) must transduce the G-CSF signal during the time lag between PI3K and p70 S6K. Chung et al. (1994) also showed a lag time between PI3K and p70 S6K activation on HepG2 cells stimulated by platelet-derived growth factor (PDGF), suggesting that some signaling molecules also may transduce between PI3K and p70S6K.

Protein kinase C (PKC) is a family of Ser/Thr kinases involved in the signal transduction pathways that are triggered by numerous extracellular and intracellular stimuli. The PKC family has been shown to play an essential role in cellular functions, including mitogenic signaling, cytoskeleton rearrangement, glucose metabolism, differentiation, and the regulation of cell survival and apoptosis. Eleven different members of the PKC family have been identified so far. Based on their structural similarities and cofactor requirements, they have been grouped into three subfamilies: (1) the classical or conventional PKCs (cPKCα, β$_1$, β$_2$, and γ), activated by Ca^{2+}, diacylglycerol, and phosphatidyl-serine; (2) the novel PKCs (nPKCδ, ε, η, and θ), which are independent of Ca^{2+} but still responsive to diacylglycerol; and (3) the atypical PKCs (aPKCζ and ι/λ), where PKCλ is the homologue of human PKCι. Atypical PKCs differ significantly from all other PKC family

members in their regulatory domains, in that they lack both the calcium-binding domain and one of the two zinc finger motifs required for diacylglycerol binding (Liu and Heckman, 1998). Romanelli et al. (1999) reported that p70 S6K is regulated by PKCζ and participates in a PI3K-regulated signaling complex. On the other hand, Selbie et al. (1993) reported that the tissue distribution of PKCζ is different from that of PKCι/λ, and that PKCι/λ appears to be widely expressed. If the p70 S6K could be activated by aPKC, the regulation of p70 S6K activation would seem to depend on the tissue-specific expression of PKCι and/or PKCζ. In neutrophilic lineage cells, the question is which aPKC participates in the regulation of p70 S6K on G-CSF signaling.

In this study, we show that G-CSF activated PKCι, promoting its translocation from the nucleus to the cell surface membrane and subsequently to the cytosol in DMSO-treated HL-60 cells. We also show the translocation of PKCι using myeloperoxidase-positive neutrophilic lineage differentiated from cord blood, which is a rich source of immature myeloid cells (Fritsch et al., 1993; Rappold et al., 1997; Huang et al., 1999; Debili et al., 2001; Hao et al., 2001). We concluded that PKCι translocation and activation by G-CSF are needed for neutrophilic proliferation.

Materials and Methods

Reagents

Anti-p70 S6K polyclonal antibody was obtained from Santa Cruz Biotechnology (Santa Cruz, CA). Anti-PKCι polyclonal antibody and monoclonal antibody were purchased from Santa Cruz Biotechnology and from Transduction Laboratories (Lexington, KY), respectively. Anti-PKCζ polyclonal antibody was purchased from Cell Signaling Technology (Beverly, MA). Anti-myeloperoxidase antibody was purchased from Serotec Ltd. (Oxford, UK). GF 109203X, and Gö 6983 were obtained from Calbiochem-Novabiochem (San Diego, CA). Wortmannin was obtained from Sigma Chemical (St. Louis, MO). Anti-Histon-H1 antibody, anti-Fcγ receptor IIa (CD32) antibody, and anti-lactate dehydrogenase antibody were from Upstate Cell Signaling Solutions (Lake Placid, NY), Lab Vision Corp. (Fremont, CA), and Chemicon International, Inc. (Temecula, CA), respectively.

Cell culture

HL-60, Jurkut, K562, U937, and THP-1 cells were kindly supplied by the Japanese Collection of Research Bioresources Cell Bank (Osaka, Japan). Cells were maintained in RPMI 1640 medium containing 10% heat-inactivated FBS and 30 mg/L kanamycin sulfate at 37°C in moisturized air containing 5% CO_2. The HL-60 cells, which were at a density of 2.5×10^5 cells/ml, were differentiated by 1.25% DMSO. Two days after the addition of DMSO, the G-CSF-induced signal transduction was analyzed using either magnetically sorted cells or non-sorted cells.

Magnetic cell sorting

To prepare Trf-R⁻ and Trf-R⁺ cells, magnetic cell sorting was performed as previously reported (Kanayasu-Toyoda et al., 2002), using an automatic cell sorter (AUTO MACS; Miltenyi Biotec, Bergisch Gladbach, Germany). After cell sorting, both cell types were used for Western blotting and PKCι enzyme activity analyses.

Preparation of cell lysates and immunoblotting

For analysis of PKCι and PKCζ expression, a PVDF membrane blotted with 50 μg of various tissues per lane was purchased from BioChain Institute (Hayward, CA). Both a polymorphonuclear leukocytes (PMNs) fraction and a fraction containing lymphocytes and monocytes were isolated by centrifugation (400g, 25 min) using a Mono-poly resolving medium (Dai-Nippon Pharmaceutical, Osaka, Japan) from human whole blood, which was obtained from a healthy volunteer with informed consent. T-lymphocytes were further isolated from the mixture fraction using the Pan T Cell Isolation Kit (Miltenyi Biotec) according to the manufacturer's protocol. T-lymphocytes, PMNs, HL-60 cells, Jurkut cells, K562 cells, and U937 cells (1×10^7) were

collected and lysed in lysis buffer containing 1% Triton X-100, 10 mM K_2HPO_4/KH_2PO_4 (pH 7.5), 1 mM EDTA, 5 mM EGTA, 10 mM $MgCl_2$, and 50 mM β-glycerophosphate, along with 1/100 (v/v) protease inhibitor cocktail (Sigma Chemical) and 1/100 (v/v) phosphatase inhibitor cocktail (Sigma Chemical). The cellular lysate of 10^6 cells per lane was subjected to Western blotting analysis. Human cord blood was kindly supplied from the Metro Tokyo Red Cross Cord Blood Bank (Tokyo, Japan) with informed consent. Mononuclear cells, isolated with the Lymphoprep™ Tube (Axis-Shield PoC AS, Oslo, Norway), were cultured in RPMI 1640 medium containing 10% FBS in the presence of G-CSF for 3 days. Cultured cells were collected, and the cell lysate was subjected to Western blotting analysis.

A fraction of the plasma membrane, cytosol, and nucleus of the DMSO-treated HL-60 cells was prepared by differential centrifugation after the addition of G-CSF, as described previously (Yamaguchi et al., 1999). After the cells that had been suspended in 250 mM sucrose/10 mM Tris-HCl (pH 7.4) containing 1/100 (v/v) protease inhibitor cocktail (Sigma Chemical) were gently disrupted by freezing and thawing, they were centrifuged at 800g, 4°C for 10 min. The precipitation was suspended in 10 mM Tris-HCl (pH 6.7) supplemented with 1% SDS. It was then digested by benzon nuclease at 4°C for 1 h and used as a sample of the nuclear fraction. After the post-nucleus supernatant was re-centrifuged at 100,000 rpm (452,000g) at a temperature of 4°C for 40 min, the precipitate was used as a crude membrane fraction and the supernatant as a cytosol fraction. Western blotting analysis was then performed as described previously (Kanayasu-Toyoda et al., 2002). The bands that appeared on x-ray films were scanned, and the density of each band was quantitated by Scion Image (Scion, Frederick, MD) using the data from three separate experiments.

Kinase assay

The activity of PKCι was determined by phosphorous incorporation into the fluorescence-labeled pseudosubstrate (Pierce Biotechnology, Rockford, IL). The cell lysates were prepared as described above and immunoprecipitated with the anti-PKCι antibody. Kinase activity was measured according to the manufacturer's protocol. In the analysis of inhibitors effects, cells were pretreated with a PI3K inhibitor, wortmannin (100 nM), or PKC inhibitors, GF109207X (10 μM) and Gö6983 (10 μM) for 30 min, and then stimulated by G-CSF for 15 min.

Observation of confocal laser-scanning microscopy

Upon the addition of G-CSF, PKCι localization in the DMSO-treated HL-60 cells for 2 days was examined by confocal laser-activated microscopy (LSM 510, Carl Zeiss, Oberkochen, Germany). The cells were treated with 50 ng/ml G-CSF for the indicated periods and then fixed with an equal volume of 4.0% paraformaldehyde in PBS(−). After treatment with ethanol, the fixed cells were labeled with anti-PKCι antibody and with secondary antibody conjugated with horseradish peroxidase. They were then visualized with TSA™ Fluorescence Systems (PerkinElmer, Boston, MA).

Mononuclear cells prepared from cord blood cells were cultured in RPMI 1640 medium containing 10% FBS in the presence of G-CSF for 7 days. Then, for serum and G-CSF starvation, cells were cultured in RPMI 1640 medium containing 1% BSA for 11 h. After stimulation by 50 ng/ml G-CSF, the cells were fixed, stained with both anti-PKCι polyclonal antibody and anti-myeloperoxidase monoclonal antibody, and finally visualized with rhodamine-conjugated anti-rabbit IgG and FITC-conjugated anti-mouse IgG, respectively.

RNA interference

Two pairs of siRNAs were chemically synthesized: annealed (Dharmacon RNA Technologies, Lafayette, CO) and transfected into HL-60 cells using Nucleofector™ (Amaxa, Cologne, Germany). The sequences of sense siRNAs were as follows: PKCι, GAAGAAGCCUUUAGACUUUTA; p70 S6K, GCAAGGAGUCUAUCCAUGAUU. As a control, the sequence ACUCUAUCGCCAGCGUGACUU was used. Forty-eight hours after treatment with siRNA, the cells were lysed for Western blot analysis. For proliferation and differentiation assay, cells were transfected with siRNA on the first day, treated with DMSO on the second day, and supplemented with G-CSF on the third day. After cells were subsequently cultured for 5 days, cell numbers and formyl-Met-Leu-Phe receptor (fMLP-R) expression were determined.

fMLP-R expression

The differentiated cells were collected and incubated with FITC-conjugated fMLP; then, labeled cells were subjected to flow cytometric analysis (FACSCalibur, Becton Dickinson, Franklin Lakes, NJ).

Statistical analysis

Statistical analysis was performed using unpaired Student's t-test. Values of $P < 0.05$ were considered to indicate statistical significance. Each experiment was repeated at least three times and representative data were indicated.

Results

The distribution of atypical PKC in various tissues and cells

Previously, we reported that the PI3K-p70 S6K-cMyc pathway plays an important role in the G-CSF-induced proliferation of DMSO-treated HL-60 cells, not only by enhancing the activity of both PI3K and p70 S6K but also by inducing the c-Myc protein (Kanayasu-Toyoda et al., 2002, 2003). We also reported that G-CSF did not stimulate Erk1, Erk2, or 4E-binding protein 1. The maximum kinase activity of PI3K was observed 5 min after the addition of G-CSF, and that of p70 S6K was observed between 30 and 60 min after. It is conceivable that any signal molecule(s) must transduce the G-CSF signal during the time lag between PI3K and p70 S6K. Romanelli et al. (1999) suggested that the activation of p70 S6K is regulated by PKCξ and participates in the PI3K-regulated signaling complex. To examine the role of atypical PKC in the G-CSF-dependent activation and the relationship between atypical PKC and p70 S6K, the protein expression of PKCξ and PKCι in various human tissues and cells was analyzed by Western blotting. As shown in Figure 1A, both of the atypical PKCs were markedly expressed in lung and kidney but were weakly expressed in spleen, stomach, and placenta. In brain, cervix, and uterus, the expression of only PKCι was observed. Selbie et al. (1993) have reported observing the expression of PKCξ not in protein levels but in RNA levels, in the kidney, brain, lung, and testis, and that of PKCι in the kidney, brain, and lung. In this study, the protein expression of PKCι in the kidney, brain, and lung was consistent with the RNA expression of PKCι. Despite the strong expression of PKCξ RNA in brain (Selbie et al., 1993), PKCξ protein was scarcely observed. Although PKCι proteins were scarcely expressed in neutrophils and T-lymphocytes in peripheral blood, they were abundantly expressed in immature blood cell lines, that is, Jurkut, K562, U937, and HL-60 cells (Fig. 1B), in contrast with the very low expression of PKCξ proteins. In mononuclear cells isolated from umbilical cord blood, which contains large numbers of immature myeloid cells and has a high proliferation ability, the expression of PKCι proteins was also observed. Since Nguyen and Dessauer (2005) have reported observing abundant PKCξ proteins in THP-1 cells, as a positive control for PKCξ, we also performed a Western blot of THP-1 cells (Fig. 1B, right part). While PKCι was markedly expressed in both THP-1 and HL-60 cells, PKCξ was observed only in THP-1 cells.

These data suggested that PKCξ and PKCι were distributed differently in various tissues and cells, and that mainly PKCι proteins were expressed in proliferating blood cells.

Stimulation of PKCι activity by G-CSF

Among the 11 different members of the PKC family, the aPKCs (ξ and ι/λ) have been reported to activate p70 S6K activity and to be regulated by PI3K (Akimoto et al., 1998; Romanelli et al., 1999). As shown in Figure 1, although the PKCξ proteins were not detected by Western blotting in HL-60 cells or mononuclear cells isolated from cord blood cells, it is possible that PKCι could functionally regulate p70 S6K as an upstream
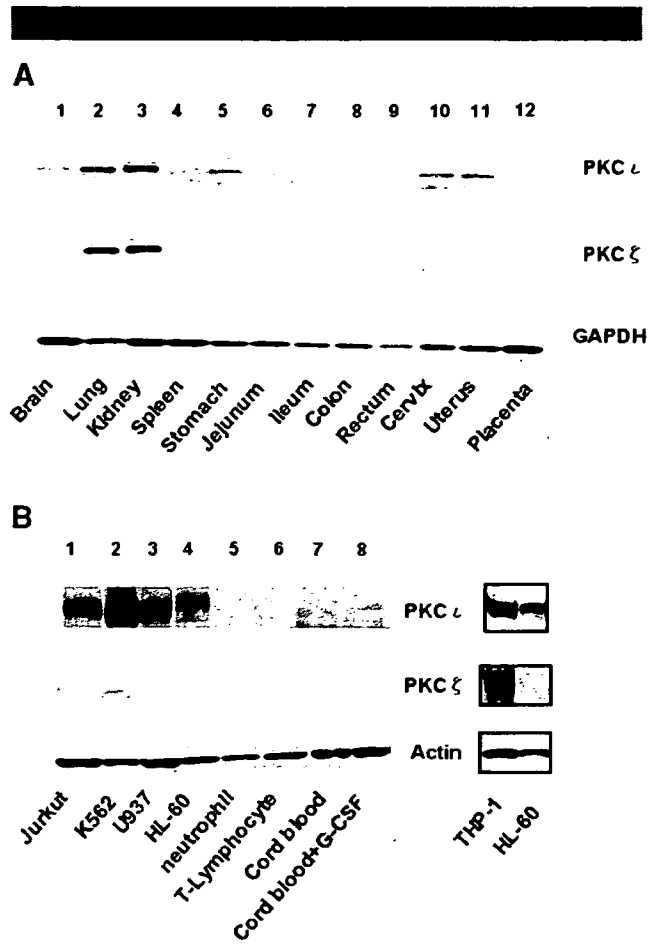
Fig. 1. Different distributions of PKCξ and PKCι. The protein expression of PKCι appears in the upper part and that of PKCξ in the middle part in various tissues and cells. A: 1, brain; 2, lung; 3, kidney, 4, spleen; 5, stomach; 6, jejunum; 7, ileum; 8, colon; 9, rectum; 10, cervix; 11, uterus; 12, placenta. Anti-GAPDH blot is a control for various tissues. B: 1, jurkut cells; 2, K562 cells; 3, U937 cells; 4, HL-60 cells; 5, neutrophils; 6, T-lymphocytes; 7, mononuclear cells from cord blood in the absence of G-CSF; 8, mononuclear cells from cord blood in the presence of G-CSF. Anti-actin blot is a control. The right part shows immunoblots of PKCι, PKCξ, and actin of THP-1 cells as a positive control for PKCξ. The cell numbers of THP-1 and HL-60 cells were adjusted in relation to other cells on the left parts.

regulator in these cells. Therefore, we focused on the role of PKCι as the possible upstream regulator of p70 S6K in neutrophil lineage cells. First, we compared the expression of PKCι in both Trf-R⁺ and Trf-R⁻ cells. PKCι proteins were expressed more abundantly in Trf-R⁺ cells than in Trf-R⁻ cells (Fig. 2A, middle part), as with the p70 S6K proteins. A time course study of PKCι activity upon the addition of G-CSF revealed the maximum stimulation at 15 min, lasting until 30 min. The G-CSF-dependent activation of PKCι was inhibited by the PKC inhibitors wortmannin, GF 109203X, and Gö 6983. Considering the marked inhibitory effect of wortmannin on PKCι and evidence that the maximum stimulation of PI3K was observed at 5 min after the addition of G-CSF, PI3K was determined to be the upstream regulator of PKCι in the G-CSF signal transduction of HL-60 cells. The basal activity of PKCι in Trf-R⁺ cells was higher than that in Trf-R⁻ cells, and G-CSF was more augmented. In Trf-R⁻ cells, PKCι activity was scarcely stimulated by G-CSF. This tendency of PKCι to be activated by G-CSF was similar to that of PI3K (Kanayasu-Toyoda et al., 2002).
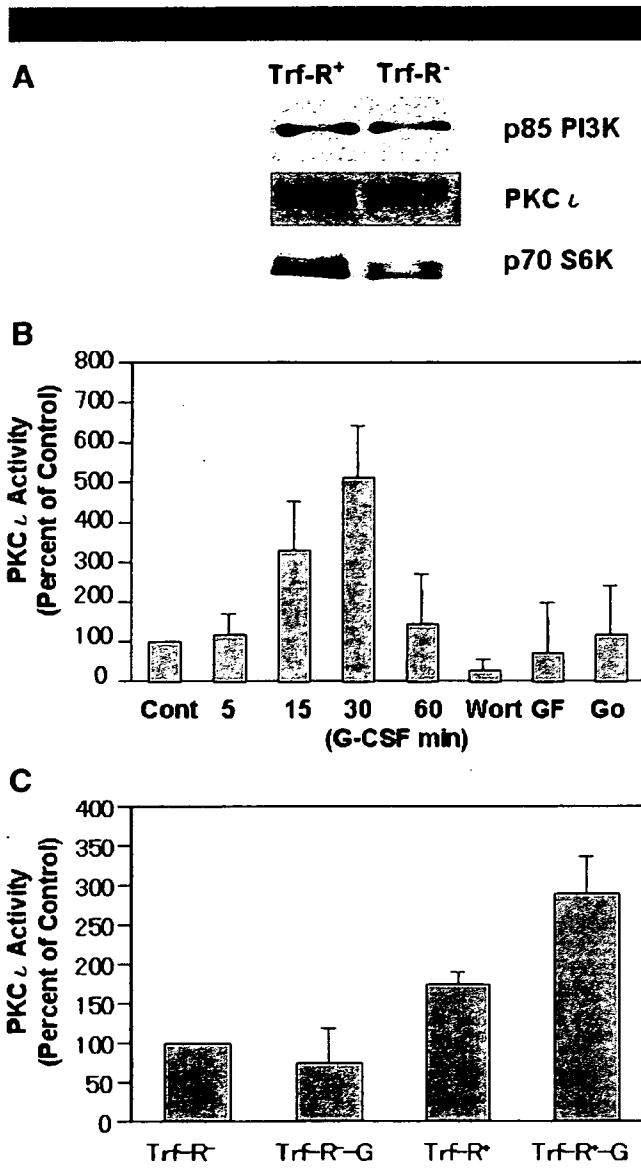
A   Trf-R⁺ Trf-R⁻

p85 PI3K

PKC ι

p70 S6K

B

C

Fig. 2.   Expression of PKCι in Trf-R⁺ and Trf-R⁻ cells and effects of G-CSF on PKCι activity. A: The expression of PKCι in Trf-R⁺ and Trf-R⁻ cells was subjected to Western blot analysis after magnetic cell sorting. B: The G-CSF-dependent PKCι activation of the DMSO-treated HL-60 cells was measured. The x-axis represents the time lapse (min) after the G-CSF stimulation and the y-axis percent of control that was not stimulated by G-CSF. Columns and bars represent the mean ± SD, using data from three separate experiments. Wort: wortmannin (100 nM), GF: GF109207X (10 μM), Gö: Gö6983 (10 μM). Cells were pretreated with each inhibitor and then stimulated by G-CSF for 15 min. C: The PKCι activity in the Trf-R⁺ and Trf-R⁻ cells 30 min after the addition of G-CSF. The y-axis represents the percentage of control that was non-stimulated Trf-R⁻ cells. Columns and bars represent the mean ± SD, using data from three separate experiments.

Effects of G-CSF on PKCι translocation

Muscella et al. (2003) demonstrated that the translocation of PKCζ from the cytosol to the nucleus or membrane is required for c-Fos synthesis induced by angiotensin II in MCF-7 cells. It was also reported that high glucose induced the translocation of PKCι (Chuang et al., 2003). These results suggest that the translocation of aPKC plays an important role in its signaling. To clarify the translocation of PKCι, immuno-histochemical staining (Fig. 3) and biochemical fractionation (Fig. 4) in

DMSO-induced HL-60 cells were performed after the addition of G-CSF. In a non-stimulated condition, PKCι in the HL-60 cells treated with DMSO for 2 days (Fig. 3, control) was detected mainly in the nucleus. Analysis of Western blotting (Fig. 4, left parts) and quantification of the bands (Fig. 4, right columns) also revealed that PKCι was localized and observed mainly in the nuclear fraction (Fig. 4A). During the 5–15 min period after the addition of G-CSF, PKCι was found to translocate (Figs. 3 and 4B) into the membrane fraction, after which it re-translocated into the cytosol fraction (Fig. 4C). In the presence of wortmannin, the G-CSF-induced translocation of PKCι into the plasma membrane failed, but PKCι was found to localize in the cytosolic fraction (Figs. 3 and 4B). Myeloperoxidase is thought to be expressed in stage from promyelocytes to mature neutrophils (Manz et al., 2002). In human cord blood cells (Fig. 3), PKCι in the cells co-stained with anti-myeloperoxidase antibody was also localized in the nucleus after serum depletion (Fig. 3B top parts). Ten minutes after the addition of G-CSF, PKCι was found to translocate into the membrane, and then into the cytosol at 30 min after the addition of G-CSF. In the presence of wortmannin, the G-CSF-induced translocation of PKCι into the plasma membrane failed but PKCι was found to localize in the cytosol. This suggested that the dynamic translocation of PKCι induced by G-CSF is a universal phenomenon in neutrophilic lineage cells. Taken together, these data support the possibility that PI3K plays not only an important role upstream of PKCι but also triggers the translocation from nucleus to membrane upon the addition of G-CSF.

In order to assess the purity of each cellular fraction, antibodies against specific markers were blotted. As specific markers, Histon-H1, Fcγ receptor IIa (CD32), and lactate dehydrogenase (LDH) were used for the nuclear, membrane, and cytosolic fractions, respectively. The purities of the nuclear, membrane, and cytosolic fractions were 82.0, 78.5, and 72.2%, respectively (Fig. 4D).

Effects of siRNA for PKCι on proliferation and differentiation

To determine the role of PKCι in neutrophilic proliferation and differentiation, PKCι was knocked down by siRNA. When the protein level of PKCι was specifically downregulated by siRNA for PKCι (Fig. 5A), G-CSF failed to enhance proliferation of the cells during 5 days' cultivation (Fig. 5B). The effect of siRNA for PKCι on neutrophilic differentiation in terms of fMLP-R expression was also determined. As shown in Figure 5C, fMLP-R expression was promoted by siRNA for PKCι in either the presence (lower part) or absence (upper part) of G-CSF. These data indicate that PKCι positively regulates G-CSF-induced proliferation and negatively regulates the differentiation of DMSO-treated HL-60 cells.

Discussion

We previously reported that PI3K/p70 S6K plays an important role in the regulation of the neutrophilic differentiation and proliferation of HL-60 cells. Akimoto et al. (1998) and Romanelli et al. (1999) reported that p70 S6K is regulated by aPKC and aPKCλ/PKCζ, respectively. At first, we showed that the distribution of PKCζ and PKCι proteins in various human tissues and cells was not similar (Fig. 1A), and that PKCι are more abundantly expressed in proliferating blood cells: Jurkut, K562, U937, and HL-60 cells (Fig. 1B). Moreover, PKCι proteins were also observed in cultured mononuclear cells of cord blood, in which the myeloid progenitors were enriched in the presence or absence of G-CSF (Fig. 1B). The myeloperoxidase-positive cells as neutrophilic lineage cells, a myeloid marker, were also stained with the antibody of PKCι (Fig. 3B). Although PKCζ proteins are barely detected in
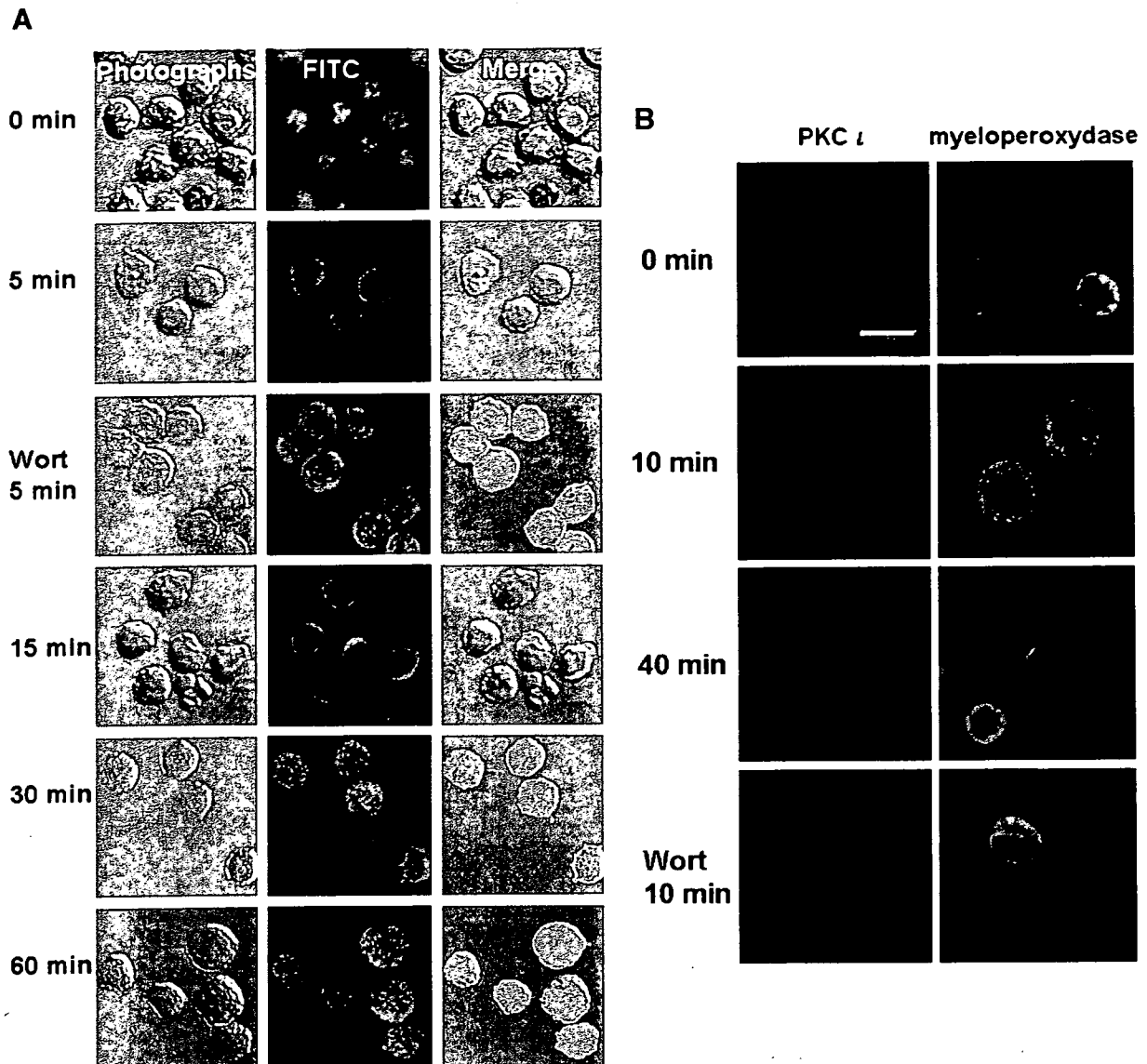
Fig. 3.   Translocation of PKCι after the activation of G-CSF. A: 2 days after the addition of DMSO, HL-60 cells stimulated by G-CSF were fixed, incubated with anti-PKCι antibody, and visualized as described above. The photographs can be seen at the left part of the figure, the fluorescent photographs in the middle of the figure, and the merged images at the right. B: G-CSF-stimulated mononuclear cells from cord blood were stained with anti-PKCι antibody (red, left part) and anti-myeloperoxidase antibody (green, right part) after serum depletion. Under no stimulation, PKCι was observed in the nucleus. G-CSF promoted the translocation of PKCι to the membrane within 5–15 min, and then to the cytosol. Wort: wortmannin. White bar: 10 μm.

neutrophilic HL-60 cells, PKCι proteins were markedly expressed in these cells (Fig. IB). This study showed, for the first time, the stimulation of PKCι activity in G-CSF-treated HL-60 cells (Fig. 2B) at 15–30 min after the addition of G-CSF. Maximum activation from the addition of NGF in PC12 cells was also observed at 15 min (Wooten et al., 2001).

Atypical PKCs are lipid-regulated kinases that need to be localized to the membrane in order to be activated. PKCζ is directly activated by phosphatidylinositol 3,4,5-trisphosphate, a product of PI3K (Nakanishi et al., 1993). We previously reported that the maximum activation of PI3K was observed in HL-60 cells 5 min after the addition of G-CSF (Kanayasu-Toyoda et al., 2002). Most investigators have reported the translocation of aPKC in either muscle cells or adipocytes stimulated by insulin (Andjelkovic et al., 1997; Goransson et al.,

1998; Galetic et al., 1999; Standaert et al., 1999; Braiman et al., 2001; Chen et al., 2003; Kanzaki et al., 2004; Sasaoka et al., 2004; Herr et al., 2005). In response to insulin stimulation, aPKCζ/λ is translocated to the plasma membrane (Standaert et al., 1999; Braiman et al., 2001), where aPKCζ/λ is believed to be activated (Galetic et al., 1999; Kanzaki et al., 2004). In the present study, the addition of G-CSF induced PKCι to translocate to the membrane from the nucleus within 5–15 min (Figs. 3 and 4), and this translocation to the plasma membrane accompanied the full activation of PKCι (Fig. 2B). Previously we reported also that the maximum activation of p70 S6K in HL-60 cells was observed from 30 to 60 min after the addition of G-CSF (Kanayasu-Toyoda et al., 1999, 2002), suggesting that there was a time lag between the activation of PI3K and p70 S6K upon the addition of G-CSF in HL-60 cells. In the present study, PKCι was
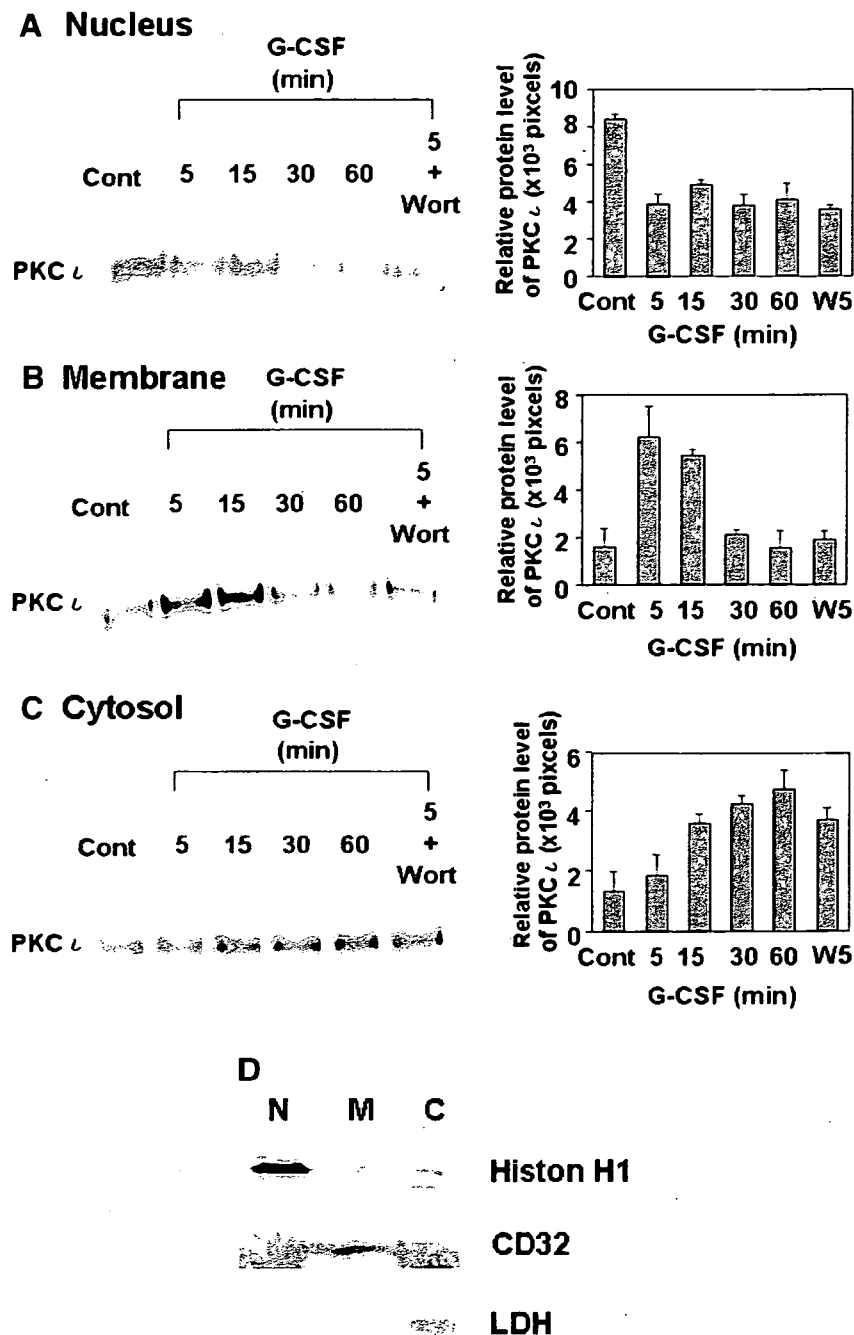
Fig. 4. Translocation of PKCι after activation by G-CSF on biochemical fractionation. The cells were differentiated as described in the Figure 3 legend. After stimulation by G-CSF, the amounts of PKCι proteins in the nucleus (A), plasma membrane (B), and cytosol (C), as fractionated by differential centrifugation, were analyzed by Western blotting (left parts). The right parts show the quantitation of the bands of PKCι proteins. Wort or W: wortmannin. PKCι protein was quantitated using data from three separate experiments. Columns and bars represent the mean ± SD. D: Each cell fraction was immunoblotted with antibodies of specific marker. Histon-H1, Fcγ receptor IIa (CD32), and lactate dehydrogenase (LDH) are specific markers for nuclear (N), membrane (M), and cytosolic (C) fractions, respectively.

found to re-translocate from the plasma membrane to the cytosol (Figs. 3 and 4C). In the presence of wortmannin, an inhibitor of PI3K, PKCι failed to translocate into the plasma membrane, but instead translocated to cytosol directly from the nucleus upon the addition of G-CSF (Figs. 3 and 4B). PKCι translocation was also observed in myeloperoxidase-positive cells derived from human cord blood (Fig. 3B), indicating that G-CSF-induced dynamic translocation of PKCι occurred in not

only a limited cell line but also neutrophilic lineage cells. These data suggest that PI3K plays an important role in the activation and translocation of PKCι during the G-CSF-induced activation of myeloid cells. Furthermore, the translocation to the plasma membrane in response to G-CSF is wortmannin sensitive, but the translocation from the nucleus upon G-CSF stimulation is not affected by wortmannin, suggesting that the initial signal of G-CSF-induced PKCι translocation from the nucleus may be
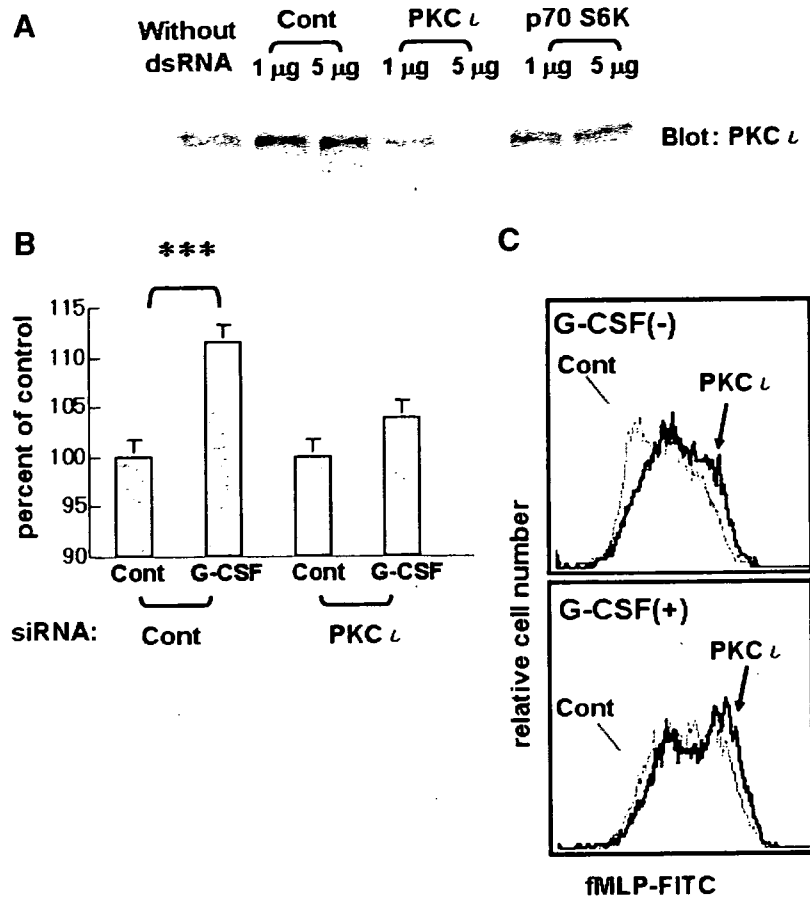
Fig. 5.   Effects of siRNA of PKCι on proliferation, differentiation, and phosphorylation at various sites of p70 S6K. A: Forty-eight hours after transfection with siRNA of PKCι or p70 S6K, protein levels of PKCι were compared. B: Proliferation of the cells transfected with siRNA of PKCι or control (Cont) was measured 5 days after the addition of G-CSF. Columns and bars represent the mean ± SD of triplicate wells ($^{***}P < 0.001$). C: fMLP-R expression was analyzed by flow cytometry 5 days after the addition of G-CSF. The gray arrow indicates cells transfected with the control sequence of double-stranded RNA (Cont, gray lines), and the black arrow the cells transfected with siRNA for PKCι (black lines) in the presence (lower part) or absence (upper part) of G-CSF.

PI3K-independent, but association of PKCι with the plasma membrane could be mediated through a PI3K-dependent signal. Cord blood is an important material of blood transplantation for leukemia (Bradstock et al., 2006; Ooi, 2006; Yamada et al., 2006) or for congenital neutropenia (Mino et al., 2004; Nakazawa et al., 2004) because it contains many hematopoietic stem cells such as CD34-positive cells or CD133-positive cells, and also contains immature granulocytes. The neutrophilic differentiation and proliferation are necessary processes after transplantation.

Formyl-Met-Leu-Phe peptide evokes the migration, superoxide production, and phagocytosis of neutrophils through fMLP-R, a suitable marker for neutrophilic differentiation. In this study, the reduction of PKCι by siRNA inhibited G-CSF-induced proliferation (Fig. 5B) and promoted neutrophilic differentiation (Fig. 5C) in terms of fMLP-R expression. These data, however, suggest that PKCι promoted G-CSF-induced proliferation and blocked differentiation at the same time. The substrates of aPKC have recently been reported: namely, the cytoskeletal protein Lethal giant larvae (Lgl) was phosphorylated by Drosophila aPKC (Betschinger et al., 2003) and glyceraldehydes-3-phosphate dehydrogenase (GAPDH) was phosphorylated by PKCι (Tisdale, 2002) directly in both cases. While the direct phosphorylation of p70 S6K by aPKC was not observed (Akimoto et al., 1998; Romanelli et al.,

1999), the enzyme activity of p70 S6K was markedly enhanced by co-transfection with aPKC and PDK-1, the latter of which is recruited to the membrane due to the binding of phosphatidylinositol-3,4,5-trisphosphate to its PH domain (Anderson et al., 1998). The addition of G-CSF induced PKCι to increase phosphorylation at Thr-389, which is the site most closely related to enzyme activity among the multi-phosphorylation sites of p70 S6K (Weng et al., 1998). However, the mammalian target of rapamycin (mTOR), an upstream regulator, also phosphorylates Thr-389 of p70 S6K and markedly stimulates p70 S6K activity under coexistence with PDK-1 (Isotani et al., 1999). We could not rule out the possibility that other PKC isoforms can contribute to the activation of p70 S6K. We postulated that in G-CSF-stimulated HL-60 cells, PKCι contributes to p70 S6K activation as an upstream regulator.

Atypical PKC isoforms are reported to play an important role in the activation of IκB kinase β (Lallena et al., 1999). In PKCζ-deficient mice, impaired signaling through the B-cell receptor resulted in the inhibition of cell proliferation and survival while also causing defects in the activation of ERK and the transcription of NF-κB-dependent genes (Martin et al., 2002). Moreover, Lafuente et al. (2003) demonstrated that the loss of Par-4, that is, the genetic inactivation of the aPKC inhibitor, led to an increased proliferative response of

peripheral T cells when challenged through the T-cell receptor. However, it has been reported that PKCλ-deficient mice have a lethal phenotype at the early embryonic stage (Soloff et al., 2004). Based on the present results and those of previous reports (Kanayasu-Toyoda et al., 1999, 2002), we postulate that PKCι plays an important role in regulating G-CSF-induced proliferation in neutrophilic lineage cells.

Acknowledgments

Literature Cited

Akimoto K, Nakaya M, Yamanaka T, Tanaka J, Matsuda S, Weng QP, Avruch J, Ohno S. 1998. Atypical protein kinase Clambda binds and regulates p70 S6 kinase. Biochem J 335:417–424.

Anderson KE, Coadwell J, Stephens LR, Hawkins PT. 1998. Translocation of PDK-1 to the plasma membrane is important in allowing PDK-1 to activate protein kinase B. Curr Biol 8:684–691.

Andjelkovic M, Alessi DR, Meier R, Fernandez A, Lamb NJ, Frech M, Cron P, Cohen P, Lucocq JM, Hemmings BA. 1997. Role of translocation in the activation and function of protein kinase B. J Biol Chem 272:31515–31524.

Betschinger J, Mechtler K, Knoblich JA. 2003. The Par complex directs asymmetric cell division by phosphorylating the cytoskeletal protein Lgl. Nature 422:326–330.

Bradstock KF, Hertzberg MS, Kerridge IH, Svennilson J, McGurgan M, Huang G, Antonenas V, Gottlieb DJ. 2006. Unrelated umbilical cord blood transplantation for adults with haematological malignancies: Results from a single Australian centre. Intern Med J 36:355–361.

Braiman L, Alt A, Kuroki T, Ohba M, Bak A, Tennenbaum T, Sampson SR. 2001. Activation of protein kinase C zeta induces serine phosphorylation of VAMP2 in the GLUT4 compartment and increases glucose transport in skeletal muscle. Mol Cell Biol 21:7852–7861.

Chen X, Al-Hasani H, Olausson T, Wenthzel AM, Smith U, Cushman SW. 2003. Activity, phosphorylation state and subcellular distribution of GLUT4-targeted Akt2 in rat adipose cells. J Cell Sci 116:3511–3518.

Chuang LY, Guh JY, Liu SF, Hung MY, Liao TN, Chiang TA, Huang JS, Huang YL, Lin CF, Yang YL. 2003. Regulation of type II transforming-growth-factor-beta receptors by protein kinase C iota. Biochem J 375:385–393.

Chung J, Grammer TC, Lemon KP, Kazlauskas A, Blenis J. 1994. PDGF- and insulin-dependent p70 S6K activation mediated by phosphatidylinositol-3-OH kinase. Nature 370:71–75.

Debili N, Robin C, Schiavon V, Letestu R, Pflumio F, Mitjavila-Garcia MT, Coulombel L, Vainchenker W. 2001. Different expression of CD41 on human lymphoid and myeloid progenitors from adults and neonates. Blood 97:2023–2030.

Fritsch G, Buchinger P, Printz D, Fink FM, Mann G, Peters C, Wagner T, Adler A, Gadner H. 1993. Rapid discrimination of early CD34+ myeloid progenitors using CD45-RA analysis. Blood 81:2301–2309.

Galetic I, Andjelkovic M, Meier R, Brodbeck D, Park J, Hemmings BA. 1999. Mechanism of protein kinase B activation by insulin/insulin-like growth factor-1 revealed by specific inhibitors of phosphoinositide 3-kinase—Significance for diabetes and cancer. Pharmacol Ther 82:409–425.

Goransson O, Wijkander J, Manganiello V, Degerman E. 1998. Insulin-induced translocation of protein kinase B to the plasma membrane in rat adipocytes. Biochem Biophys Res Commun 246:249–254.

Hao QL, Zhu J, Price MA, Payne KJ, Barsky LW, Crooks GM. 2001. Identification of a novel, human multilymphoid progenitor in cord blood. Blood 97:3683–3690.

Herr HJ, Bernard JR, Reeder DW, Rivas DA, Limon JJ, Yaspelkis BB3rd. 2005. Insulin-stimulated plasma membrane association and activation of Akt2, aPKC zeta and aPKC lambda in high fat fed rodent skeletal muscle. J Physiol 565:627–636.

Huang S, Chen Z, Yu JF, Young D, Bashey A, Ho AD, Law P. 1999. Correlation between IL-3 receptor expression and growth potential of human CD34+ hematopoietic cells from different tissues. Stem Cells 17:265–272.

Isotani S, Hara K, Tokunaga C, Inoue H, Avruch J, Yonezawa K. 1999. Immunopurified mammalian target of rapamycin phosphorylates and activates p70 S6 kinase alpha in vitro. J Biol Chem 274:34493–34498.

Kanayasu-Toyoda T, Yamaguchi T, Uchida E, Hayakawa T. 1999. Commitment of neutrophilic differentiation and proliferation of HL-60 cells coincides with expression of transferrin receptor. Effect of granulocyte colony stimulating factor on differentiation and proliferation. J Biol Chem 274:25471–25480.

Kanayasu-Toyoda T, Yamaguchi T, Oshizawa T, Kogi M, Uchida E, Hayakawa T. 2002. Role of the p70 S6 kinase cascade in neutrophilic differentiation and proliferation of HL-60 cells—a study of transferrin receptor-positive and -negative cells obtained from dimethyl sulfoxide- or retinoic acid-treated HL-60 cells. Arch Biochem Biophys 405:21–31.

Kanayasu-Toyoda T, Yamaguchi T, Oshizawa T, Uchida E, Hayakawa T. 2003. The role of c-Myc on granulocyte colony-stimulating factor-dependent neutrophilic proliferation and differentiation of HL-60 cells. Biochem Pharmacol 66:133–140.

Kanzaki M, Mora S, Hwang JB, Saltiel AR, Pessin JE. 2004. Atypical protein kinase C (PKCzeta/lambda) is a convergent downstream target of the insulin-stimulated phosphatidylinositol 3-kinase and TC10 signaling pathways. J Cell Biol 164:279–290.

Lafuente MJ, Martin P, Garcia-Cao I, Diaz-Meco MT, Serrano M, Moscat J. 2003. Regulation of mature T lymphocyte proliferation and differentiation by Par-4. Embo J 22:4689–4698.

Lallena MJ, Diaz-Meco MT, Bren G, Paya CV, Moscat J. 1999. Activation of IkappaB kinase beta by protein kinase C isoforms. Mol Cell Biol 19:2180–2188.

Liu WS, Heckman CA. 1998. The sevenfold way of PKC regulation. Cell Signal 10:529–542.

Manz MG, Miyamoto T, Akashi K, Weissman IL. 2002. Prospective isolation of human clonogenic common myeloid progenitors. Proc Natl Acad Sci USA 99:11872–11877.

Martin P, Duran A, Minguet S, Gaspar ML, Diaz-Meco MT, Rennert P, Leitges M, Moscat J. 2002. Role of zeta PKC in B-cell signaling and function. Embo J 21:4049–4057.

Mino E, Kobayashi R, Yoshida M, Suzuki Y, Yamada M, Kobayashi K. 2004. Umbilical cord blood stem cell transplantation from unrelated HLA-matched donor in an infant with severe congenital neutropenia. Bone Marrow Transplant 33:969–971.

Muscella A, Greco S, Elia MG, Storelli C, Marsigliante S. 2003. PKC-zeta is required for angiotensin II-induced activation of ERK and synthesis of C-FOS in MCF-7 cells. J Cell Physiol 197:61–68.

Nakanishi H, Brewer KA, Exton JH. 1993. Activation of the zeta isozyme of protein kinase C by phosphatidylinositol 3,4,5-trisphosphate. J Biol Chem 268:13–16.

Nakazawa Y, Sakashita K, Kinoshita M, Saida K, Shigemura T, Yanagisawa R, Shikama N, Kamijo T, Koike K. 2004. Successful unrelated cord blood transplantation using a reduced-intensity conditioning regimen in a 6-month-old infant with congenital neutropenia complicated by severe pneumonia. Int J Hematol 80:287–290.

Nguyen BT, Dessauer CW. 2005. Relaxin stimulates protein kinase C zeta translocation: Requirement for cyclic adenosine 3',5'-monophosphate production. Mol Endocrinol 19:1012–1023.

Ooi J. 2006. The efficacy of unrelated cord blood transplantation for adult myelodysplastic syndrome. Leuk Lymphoma 47:599–602.

Rappold I, Ziegler BL, Kohler I, Marchetto S, Rosnet O, Birnbaum D, Simmons PJ, Zannettino AC, Hill B, Neu S, Knapp W, Alitalo R, Alitalo K, Ullrich A, Kanz L, Buhring HJ. 1997. Functional and phenotypic characterization of cord blood and bone marrow subsets expressing FLT3 (CD135) receptor tyrosine kinase. Blood 90:111–125.

Romanelli A, Martin KA, Toker A, Blenis J. 1999. p70 S6 kinase is regulated by protein kinase Czeta and participates in a phosphoinositide 3-kinase-regulated signalling complex. Mol Cell Biol 19:2921–2928.

Sasaoka T, Wada T, Fukui K, Murakami S, Ishihara H, Suzuki R, Tobe K, Kadowaki T, Kobayashi M. 2004. SH2-containing inositol phosphatase 2 predominantly regulates Akt2, and not Akt1, phosphorylation at the plasma membrane in response to insulin in 3T3-L1 adipocytes. J Biol Chem 279:14835–14843.

Selbie LA, Schmitz-Peiffer C, Sheng Y, Biden TJ. 1993. Molecular cloning and characterization of PKC iota, an atypical isoform of protein kinase C derived from insulin-secreting cells. J Biol Chem 268:24296–24302.

Soloff RS, Katayama C, Lin MY, Feramisco JR, Hedrick SM. 2004. Targeted deletion of protein kinase C lambda reveals a distribution of functions between the two atypical protein kinase C isoforms. J Immunol 173:3250–3260.

Standaert ML, Bandyopadhyay G, Perez L, Price D, Galloway L, Poklepovic A, Sajan MP, Cenni V, Sirri A, Moscat J, Toker A, Farese RV. 1999. Insulin activates protein kinases C-zeta and C-lambda by an autophosphorylation-dependent mechanism and stimulates their translocation to GLUT4 vesicles and other membrane fractions in rat adipocytes. J Biol Chem 274:25308–25316.

Tenen DG, Hromas R, Licht JD, Zhang DE. 1997. Transcription factors, normal myeloid development, and leukemia. Blood 90:489–519.

Tisdale EJ. 2002. Glyceraldehyde-3-phosphate dehydrogenase is phosphorylated by protein kinase Ciota/lambda and plays a role in microtubule dynamics in the early secretory pathway. J Biol Chem 277:3334–3341.

Ward AC, Loeb DM, Soede-Bobok AA, Touw IP, Friedman AD. 2000. Regulation of granulopoiesis by transcription factors and cytokine signals. Leukemia 14:973–990.

Weng QP, Kozlowski M, Belham C, Zhang A, Comb MJ, Avruch J. 1998. Regulation of the p70 S6 kinase by phosphorylation in vivo. Analysis using site-specific anti-phosphopeptide antibodies. J Biol Chem 273:16621–16629.

Wooten MW, Vandenplas ML, Seibenhener ML, Geetha T, Diaz-Meco MT. 2001. Nerve growth factor stimulates multisite tyrosine phosphorylation and activation of the atypical protein kinase C's via a src kinase pathway. Mol Cell Biol 21:8414–8427.

Yamada K, Mizusawa M, Harima A, Kajiwara K, Hamaki T, Hoshi K, Kozai Y, Kodo H. 2006. Induction of remission of relapsed acute myeloid leukemia after unrelated donor cord blood transplantation by concomitant low-dose cytarabine and calcitriol in adults. Eur J Haematol 77:345–348.

Yamaguchi T, Mukasa T, Uchida E, Kanayasu-Toyoda T, Hayakawa T. 1999. The role of STAT3 in granulocyte colony-stimulating factor-induced enhancement of neutrophilic differentiation of Me2SO-treated HL-60 cells. GM-CSF inhibits the nuclear translocation of tyrosine-phosphorylated STAT3. J Biol Chem 274:15575–15581.

ELSEVIER

Study on the quality control of cell therapy products Determination of N-glycolylneuraminic acid incorporated into human cells by nano-flow liquid chromatography/Fourier transformation ion cyclotron mass spectrometry

Noritaka Hashii [a,b], Nana Kawasaki [a,b,*], Yukari Nakajima [a,b], Masashi Toyoda [c],
Yoko Katagiri [c], Satsuki Itoh [a], Akira Harazono [a],
Akihiro Umezawa [c], Teruhide Yamaguchi [a]

[a] *Division of Biological Chemistry and Biologicals, National Institute of Health Sciences, 1-18-1 Kamiyouga, Setagaya-ku, Tokyo 158-8501, Japan*
[b] *Core Research for Evolutional Science and Technology (CREST) of Japan Science and Technology Agency (JST),
4-1-8 Hon-cho, Kawaguchi, Saitama 332-0012, Japan*
[c] *National Research Institute for Child Health and Development, 2-10-1 Okura, Setagaya-ku, Tokyo 157-8535, Japan*

Abstract

N-Glycolylneuraminic acid (NeuGc), an acidic nine-carbon sugar, is produced in several animals, such as cattle and mice. Since human cells cannot synthesize NeuGc, it is considered to be immunogenic in humans. Recently, NeuGc contamination was reported in human embryonic stem cells cultured with xenogeneic serum and cells, suggesting that possibly NeuGc may harm the efficacy and safety of cell therapy products. Sialic acids have been determined by derivatization with 1,2-diamino-4,5-methylenedioxybenzene (DMB) followed by liquid chromatography/mass spectrometry (LC/MS) and liquid chromatography/tandem mass spectrometry (LC/MS/MS); however, the limited availability of cell therapy products requires more sensitive and specific methods for the quality test. Here we studied the use of nano-flow liquid chromatography/Fourier transformation ion cyclotron resonance mass spectrometry (nanoLC/FTMS) and nanoLC/MS/MS for NeuGc-specific determination at a low femtomole level. Using our method, we found NeuGc contamination of the human cell line (HL-60RG cells) cultured with human serum. Our method needs only 2.5×10^3 cells for one injection and would be applicable to the determination of NeuGc in cell therapy products.
© 2007 Elsevier B.V. All rights reserved.

Keywords: N-Glycolylneuraminic acid; Nano-flow liquid chromatography; Fourier transformation ion cyclotron mass spectrometry; Cell therapy products

1. Introduction

Sialic acids are a family of acidic nine-carbon sugars found in the non-reducing terminal of N-linked and O-linked oligosaccharides of glycoproteins and glycolipids [1,2]. There are more than 30 members with different substitutions on the amino group at carbon 5 and on hydroxyl groups at carbons 4, 7, 8 and 9 [2–8]. N-Glycolylneuraminic acid (NeuGc), a 5-N-glycolylated sialic acid, is produced in several animals, such as cattle, horses, mice and rats [9]. Since human cells cannot

synthesize NeuGc due to mutation of the cytidine monophospho (CMP)-N-acetylneuraminic acid (NeuAc) hydroxylase gene [10,11], NeuGc is considered to be antigenic and to induce immunoreaction in humans [4,12,13].

Advances in biotechnology and cell culture techniques make it possible to administer human and animal cells directly to patients as cell therapy products. In cell therapy and tissue engineering, human embryonic stem (ES) cells are expected to be useful for the treatment of many diseases. Recently, it was reported that NeuGc is incorporated into ES cells from human and mouse feeder cells and cultivation media containing xenogeneic serum, such as fetal calf serum (FCS) [14,15]. Since NeuGc is a foreign component in humans, it is feared that NeuGc may harm the efficacy and safety of cell therapy products. To

assess the adverse effects of NeuGc, it is necessary to quantify NeuGc in cell therapy products.

Sialic acids have been determined by labeling with 1,2-diamino-4,5-methylenedioxybenzene (DMB) followed by conventional high-performance liquid chromatography (HPLC) with fluorescent detection [16–20]. The femtomole level of sialic acid can be determined by fluorescent detection [19]. The use of liquid chromatography/mass spectrometry (LC/MS) and liquid chromatography/tandem mass spectrometry (LC/MS/MS) has more advantage in the identification of sialic acid species [18,20–22]. The derivatization of sialic acids with DMB has advantages of good separation of NeuGc from NeuAc in chromatography and enhancement of ionization efficiency in MS. However, more sensitive and specific methods are desired for the quality control of cell therapy products, since in many case only a low number of cell products, approximately 1×10^6 to 1×10^8, should be available for quality tests.

In this study, we studied the use of nano-flow liquid chromatography/Fourier transformation ion cyclotron resonance mass spectrometry (nanoLC/FTMS) and LC/MS/MS to achieve the sensitive and specific determination of NeuGc. The potential of the method for quality testing of cell therapy products was evaluated using substrain of human promyelocytic leukemia HL-60 cells (HL-60RG cells) as model cells. Using this method, we determined NeuGc in membrane fractions from HL-60RG cells cultured with FCS, human serum and serum-free medium.

2. Experimental

2.1. Materials

NeuGc and NeuAc were purchased from Nacalai Tesque (Kyoto, Japan). FCS and normal human serum were purchased from Dainippon Sumitomo Pharma (Osaka, Japan). RPMI1640 medium and ASF104 medium were purchased from Sigma-Aldrich (St. Louis, MO, USA) and Ajinomoto (Tokyo, Japan), respectively.

2.2. Cell culture

Substrain of human promyelocytic leukemia HL-60 cells (HL-60RG cells, JCRB Cellbank, Osaka, Japan) was cultured in RPMI1640 medium supplemented with 10% FCS, 100 unit/ml of penicillin and 100 μg/ml of streptomycin under a humidified atmosphere of 95% air and 5% CO_2 at 37 °C. HL-60RG cells were replaced at 2×10^5 cells/100 mm dish in RPMI1640 medium supplemented with 10% FCS or 10% normal human serum, and in serum-free ASF104 medium. The media were replaced four times, and semi-confluent growth cells were harvested.

2.3. Fractionation of the membrane fraction

The cells were washed in phosphate buffer saline (PBS) supplemented with protease inhibitors (protease inhibitor mix

solution, Wako, Tokyo, Japan) three times. The washed cells (1×10^6) were suspended in 100 μl of 0.25 M sucrose/10 mM Tris-HCl buffer (pH 7.4) containing protease inhibitors, and sonicated at 4 °C for 30 s, two times (40W, Bioruptor UCW-201, Tosyoudenki, Kanagawa, Japan). After the nuclei were removed by centrifugation at 4 °C, $450 \times g$ for 10 min, the mitochondria and lysosome fractions were removed by re-centrifugation at 4 °C, $20,000 \times g$ for 10 min. The membrane fractions were precipitated by ultracentrifugation at 4 °C, $100,000 \times g$ for 60 min. The membrane fractions were washed in 100 μl of 150 mM ammonium acetate buffer (pH 7.4) and recovered by re-ultracentrifugation.

2.4. Derivatization of NeuGc and NeuAc with DMB reagent

The membrane fractions were sonicated in 250 μl of H_2O and then incubated with 250 μl of 4 M acetic acid (final concentration, 2 M) at 80 °C for 3 h. The released sialic acids were passed though a solid-phase extraction cartridge (SepPak C-18, Waters, Milford, MA, USA) with 2 ml of H_2O, dried under vacuum, and resolved in 50 μl of H_2O. The solution was incubated with DMB according to the manufacturer's instruction (Takara, Tokyo, Japan), and the reaction mixture was applied on a solid-phase extraction cartridge (Envi-Carb C, Supelco, Bellefonte, PA, USA). After washing the cartridge with 2.5 ml of 5 mM ammonium acetate (pH 9.6) for desalting, the DMB-labeled sialic acids were eluted with 3 ml of 45% acetonitrile/5 mM ammonium acetate (pH 9.6). The collected fraction was freeze dried.

2.5. nanoLC/FTMS

DMB-labeled sialic acids were separated by HPLC using Paradigm MS4 (Michrom BioResource, Auburn, CA, USA) equipped with a reversed-phase C18 column (Magic C18, 50 mm × 0.1 mm, 3 μm, Michrom BioResource, Auburn, CA, USA). Elution was achieved using 0.1% formic acid/2% ace-
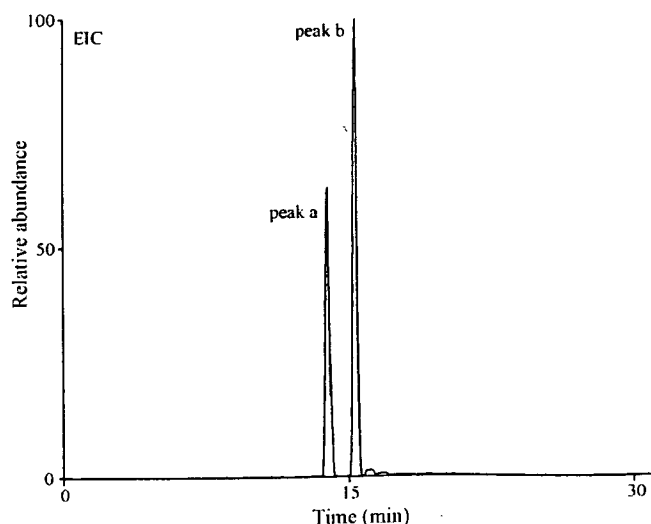

Fig. 1. EIC at m/z 426.13–426.17 and m/z 442.12–442.16 obtained by SIM (m/z 400–450) of DMB-NeuGc and DMB-NeuAc in the positive ion mode.
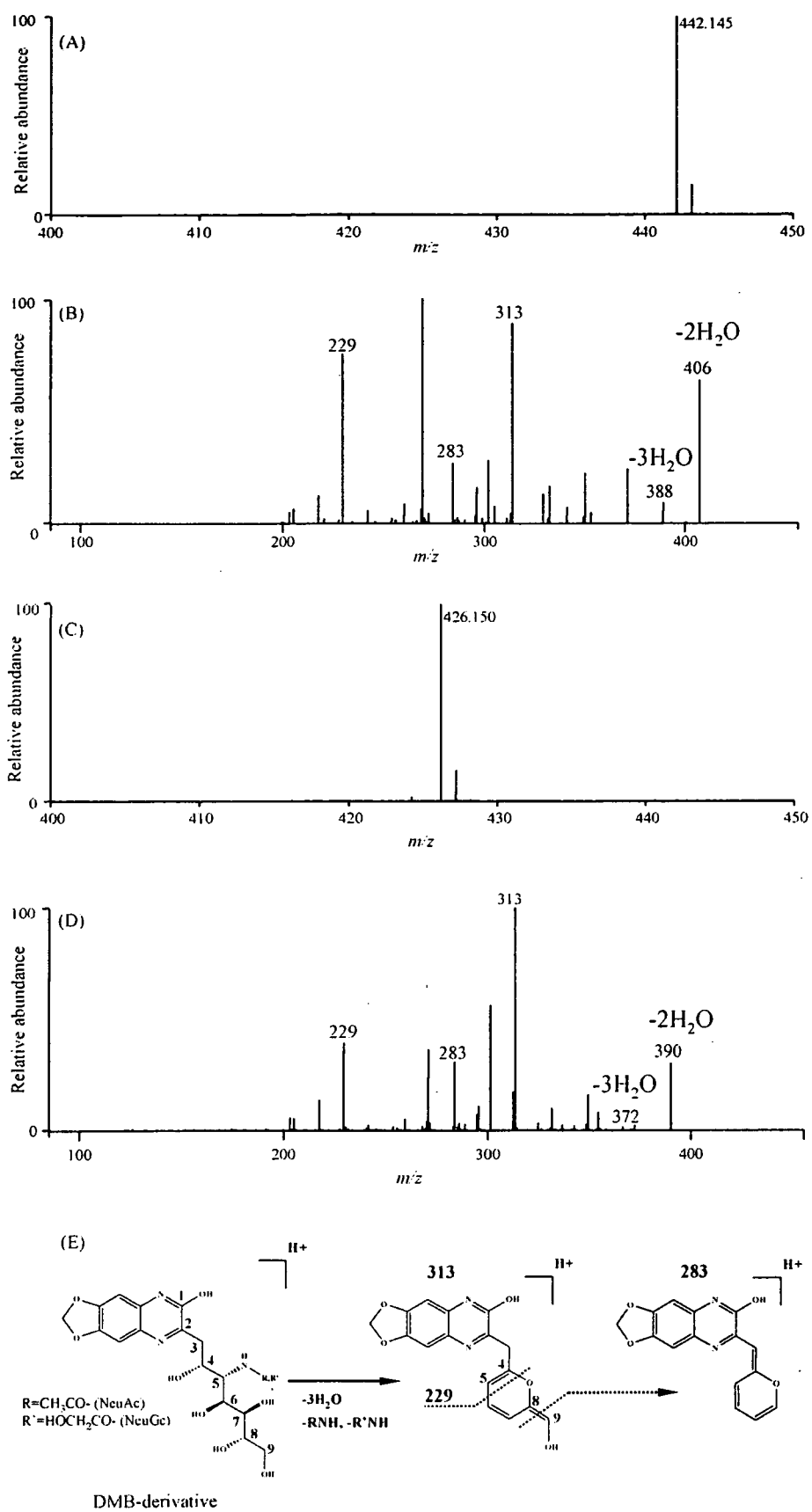
Fig. 2. (A) Typical MS spectrum of peak a. (B) MS/MS spectrum of [M + H]$^+$ (m/z 442.145) acquired from around peak a. (C) Typical MS spectrum of peak b. (D) MS/MS spectrum of [M + H]$^+$ (m/z 426.150) acquired from around peak b. (E) Fragmentation of DMB-NeuGc and DMB-NeuAc.
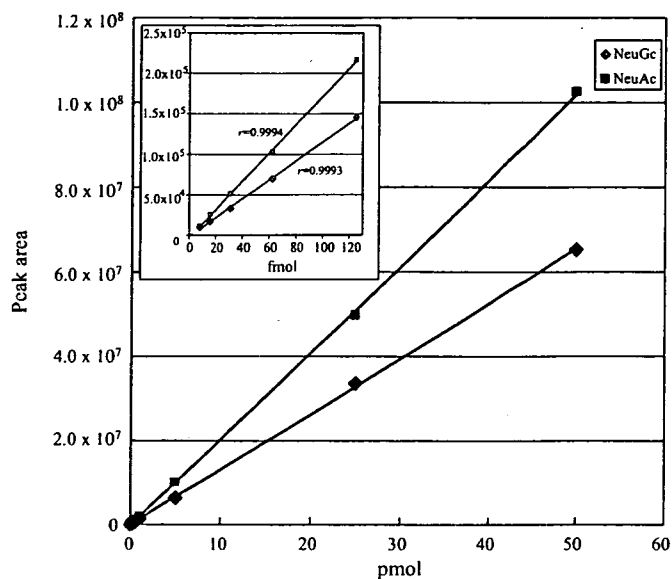
Fig. 3. Calibration curves of DMB-NeuGc ($r = 0.9998$) and DMB-NeuAc ($r = 0.9995$).

tonitrile (pump A) and 0.1% formic acid/80% acetonitrile (pump B) with a linear gradient of 10–90% of B in 30 min at a flow rate of 750 nl/min. On-line MS and MS/MS were performed using an Fourier transformation ion cyclotron resonance (FT)/ion trap (IT) type mass spectrometer (LTQ-FT, Thermo-Electron, San Jose, CA, USA) equipped with a nanoelectrospray ion source (AMR, Tokyo, Japan). DMB-NeuAc and DMB-NeuGc were determined by selected ion monitoring (SIM) in the positive ion mode. The analytical conditions were set to 200 °C for capillary temperature, 1800 eV spray voltage, m/z 400–450 scan range, and 35% collision energy. The automatic gain control (AGC) value, which is adjusted for the amount of imported ions for FTMS, was set to 5×10^4. Maximum injection times, which are the adjusted times of imported ions, for ITMS and FTMS, were set to 50 and 1250 ms, respectively.

2.6. Method validation

The linearity of the signal intensity peak area of DMB-NeuAc and DMB-NeuGc was assessed by injections of 0.0078–500 pmol DMB derivatives. Correlation coefficients were calibrated using a least-squares linear regression model. The detection limit (DL) and the quantification limit (QL) were calculated using the formulas $DL = 3.3 \times \sigma/slope$ (σ: average of noise on chromatograph) and $QL = 10 \times \sigma/slope$, respectively. Accuracy and precision were determined by measuring three samples, where NeuGc spiked at the concentration of 50 fmol to the membrane fraction of cells cultured in serum-free medium which contains no NeuGc before the derivatization of NeuGc with DMB. Accuracy was calculated by comparison of the mean peak area and the calibration curve. Precision was estimated by relative standard deviation (RSD) from three samples.
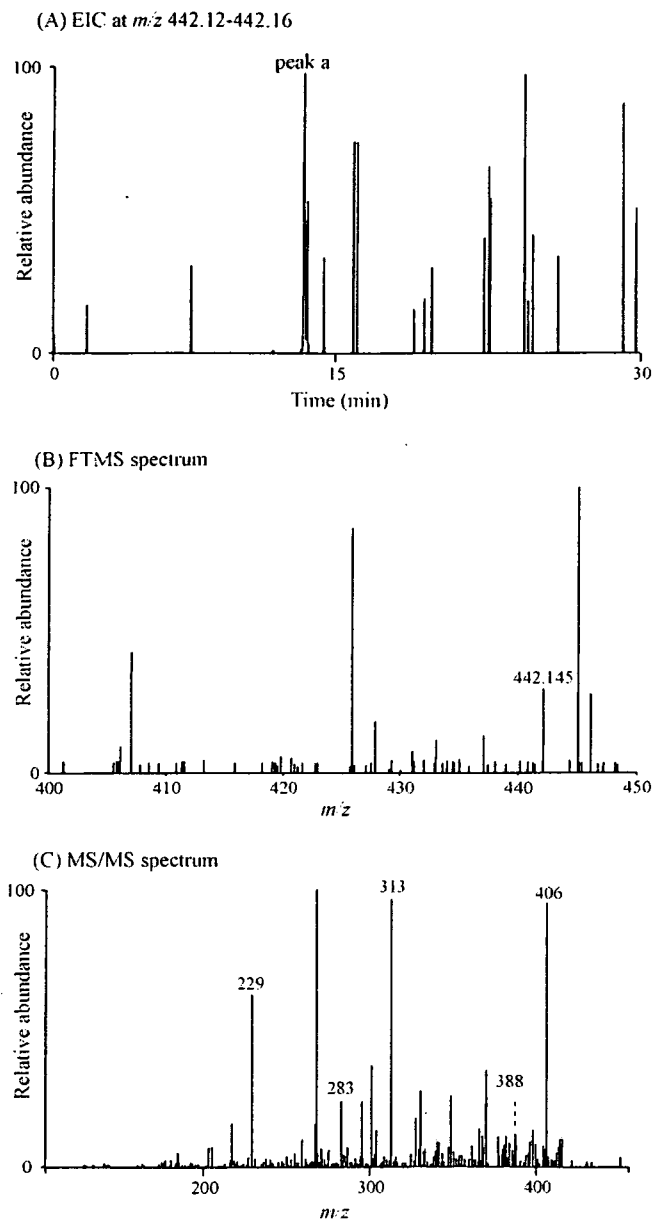

Fig. 4. Detection of DMB-NeuGc in the membrane fractions of HL-60RG cells (2.5×10^3) cultured with 10% FCS. (A) EIC at m/z 442.12–442.16 obtained by SIM. (B) Typical MS spectrum of peak a. (C) MS/MS spectrum of $[M+H]^+$ (m/z 442.145) acquired from around peak a.

3. Results and discussion

3.1. Analysis of NeuGc and NeuAc by nanoLC/FTMS

It was reported that DMB-NeuGc yielded its dehydrated ion (m/z 424) together with molecular ion (m/z 442) by MS in the positive ion mode [18,21]. To control the dehydration of molecular ion in the ion trap device, AGC value, which regulates the amount of ions trapped into ion trap device, was set to 5×10^4 (default value, 5×10^5). This value was also useful for the detection of molecular ion of DMB-NeuAc.

Using the AGC value at 5×10^4, SIM (m/z 400–450) was carried out in the positive ion mode. When a mix-
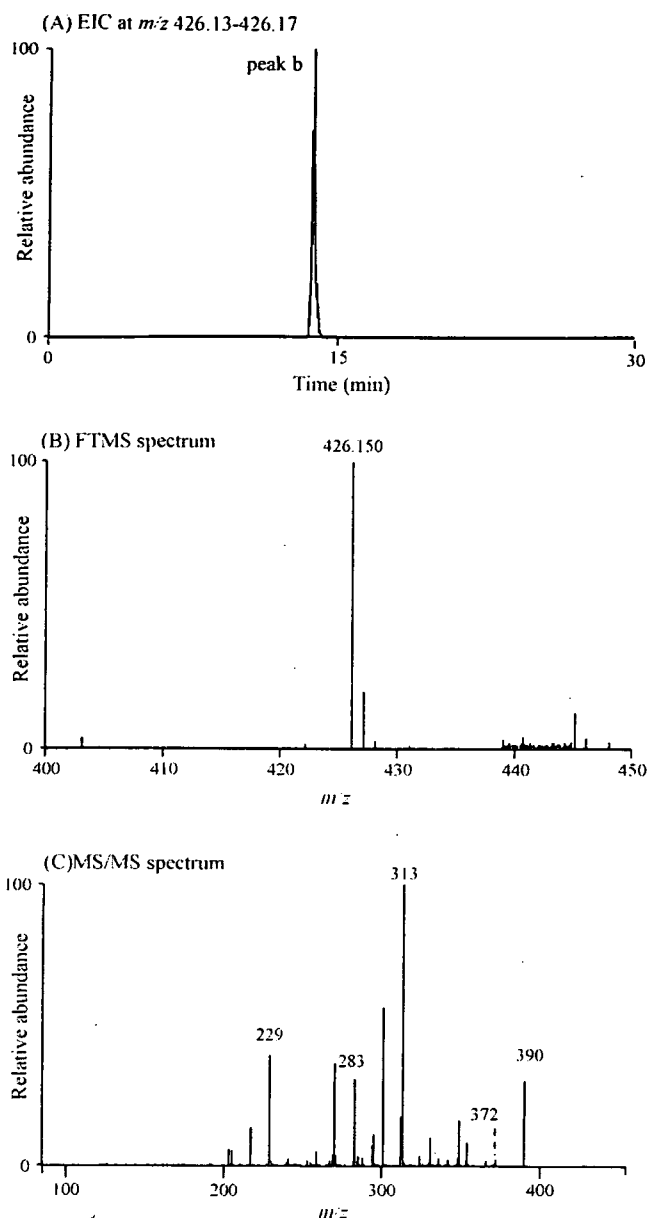
Fig. 5. Detection of DMB-NeuAc in the membrane fractions of HL-60RG cells (2.5 × 10³) cultured with 10% FCS. (A) EIC at m/z 426.13–426.17 obtained by SIM. (B) Typical MS spectrum of peak b, (C) MS/MS spectrum of [M + H]⁺ (m/z 426.150) acquired from around peak b.

Fig. 6. Levels of (A) NeuGc and (B) NeuAc in the membrane fraction of HL-60RG cells (2.5 × 10³) cultured with 10% FCS, 10% human serum (HS) and serum-free medium. Values are the means ± SD ($n = 3$).

ture of DMB-NeuGc and DMB-NeuAc (2 pmol each) was subjected to nanoLC/MS, two peaks appeared at 14 min (peak a) and 15 min (peak b) on the extracted ion chromatogram (EIC) at m/z 426.13–426.17 and m/z 442.12–442.16 (Fig. 1).

As shown in Fig. 2A, the m/z values of molecular ions around 14 min (m/z 442.145) suggest the elution of DMB-NeuGc in peak a. The structure of the DMB derivative at peak a was confirmed by the product ion spectra acquired from [M + H]⁺ (m/z 442.145) as a precursor ion (Fig. 2B). Product ions missing two and three molecules of H_2O were found at m/z 406 and 388 in MS/MS spectra. Ions losing three H_2O and glycolyl groups (m/z 313), cross-ring fragment ion (m/z 229) and fragment ion yielded by loss of formaldehyde (m/z 283) were also formed by
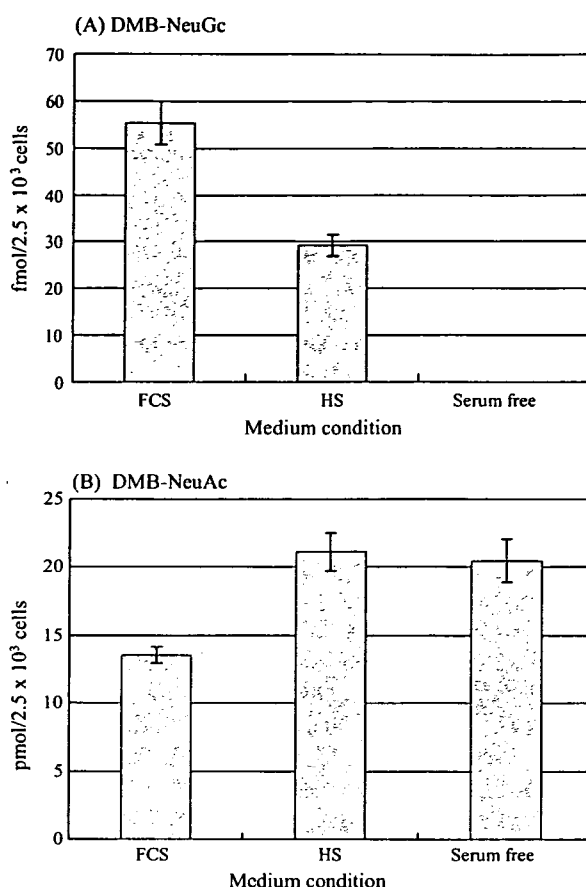
MS/MS (Fig. 2E). The fragment pattern of the MS/MS spectrum from [M + H]⁺ (m/z 442.145) was consistent with that of DMB-NeuGc in the previous report [21]. Fragments at m/z 406 and 388 are DMB-NeuGc characteristic ions, which could be used for specific determination of DMB-NeuGc. Likewise, peak b was identified as DMB-NeuAc by molecular ions (m/z 426.150) and their product ions (m/z 390, 372, 313, 283 and 229) formed by MS/MS of [M + H]⁺ (m/z 426.150) as a precursor ion (Fig. 2C and D).

Calibration curves were prepared by the injection of DMB-NeuGc and DMB-NeuAc from 0.0078 to 500 pmol. The linearity of DMB-NeuGc and DMB-NeuAc was confirmed in the range of 0.0078–50 pmol with the regression equations of $Y = 1.31 \times 10^6 X - 9028.5$ ($r = 0.9998$) and $Y = 2.03 \times 10^6 X - 21548.0$ ($r = 0.9995$), respectively (Fig. 3). DL and QL of DMB-NeuGc were 8.6 and 26.3 fmol, and those of DMB-NeuAc were 5.6 and 16.9 fmol, respectively. The use of FT/MS gave an accuracy of 92.4% by eliminating contaminants by using accurate m/z values. The precision of this method for NeuGc was 7.3%. Compared to the former method, in which a micro or semi-micro column and the quadrupole mass spectrometer were used for the detection of picomole levels of DMB derivatives, SIM by using nanoLC/FTMS achieved the specific detection of DMB-derivatized sialic acids at a lower level. The method using nanoLC/FTMS and nanoLC/MS/MS allows not

only the determination of DMB-derivatives with similar sensitivity as the fluorescence detection but also the identification of sialic acid species.

3.2. Quantification of NeuAc and NeuGc in membrane fraction of HL-60RG cells

Using HL-60RG cells as model cells, the potential of this method for the quantification of NeuGc on the cell membrane was evaluated. The membrane fraction from cells (1×10^6) cultured with 10% FCS was prepared by ultracentrifugation. Sialic acids were released by treatment with 2 M acetic acid at 80 °C for 3 h and derivatized with DMB. DMB derivatives (2.5×10^3 cells) were subjected to nanoLC/MS and nanoLC/MS/MS in SIM mode. As shown in Fig. 4A, some peaks appeared in EIC at m/z 442.12–442.16. Based on the retention time as well as the m/z value of molecular ion (m/z 442.145), peak a that appeared at 14 min was assigned to be a peak of NeuGc (Fig. 4B). Fig. 4C shows the MS/MS spectrum acquired from [M + H]+ (m/z 442.145) as precursor. The NeuGc-characteristic ions at m/z 406 and 388 together with other product ions at m/z 313, 283 and 229 clearly indicate the presence of NeuGc in the membrane fraction of HL-60RG cells. In the EIC at m/z 426.13–426.17, the single peak was observed at 15 min (Fig. 5A). The molecular ion at m/z 426.150, and product ions at m/z 390, 372, 313, 283 and 229 acquired at 15.13 min suggest that DMB-NeuAc is eluted in peak b (Fig. 5B and C). The levels of NeuGc and NeuAc in the membrane fraction from HL-60RG cells (2.5×10^3 cells) cultured with 10% FCS were 55.4 ± 4.6 fmol and 13.5 ± 0.6 pmol, respectively (Fig. 6)

After the cultivation of HL-60RG cells with human serum for 10 days (medium was changed four times), NeuGc and NeuAc were determined by the proposed method. Fig. 7A shows the EIC at m/z 442.12–442.16 obtained by nanoLC/MS. In spite of cultivation in human serum, an obvious peak still appeared at 14 min. Molecular ion (m/z 442.145) and NeuGc-characteristic product ions found in the MS/MS spectrum acquired from the molecular ion clearly indicate the presence of NeuGc in the membrane fraction (Fig. 7B and C). The levels of NeuGc and NeuAc in cells (2.5×10^3) cultured in 10% human serum were 29.2 ± 2.4 fmol and 21.0 ± 1.4 pmol, respectively (Fig. 6).

In contrast, no significant peaks appeared in EIC at m/z 442.12–442.16 when HL-60RG cells were cultured in serum-free medium for 14 days (medium was changed four times). The level of NeuAc in cells cultured in serum-free medium was 20.5 ± 1.6 pmol (Fig. 6).

As shown in Figs. 4A and 7A, there are many different molecules detected at m/z 442.14–442.16 in the cells, which makes it difficult to determine a small amount of NeuGc in the membrane fraction by the low-resolution mass spectrometry. The DMB-NeuGc-specific detection was achieved by acquisition of both the accurate mass by FTMS and the characteristic product ions arisen from DMB-NeuGc by MS/MS.

Our method needs only 2.5×10^3 cells for one injection and is applicable to the determination of NeuGc in cell therapy products. The incorporation of dietary NeuGc into human
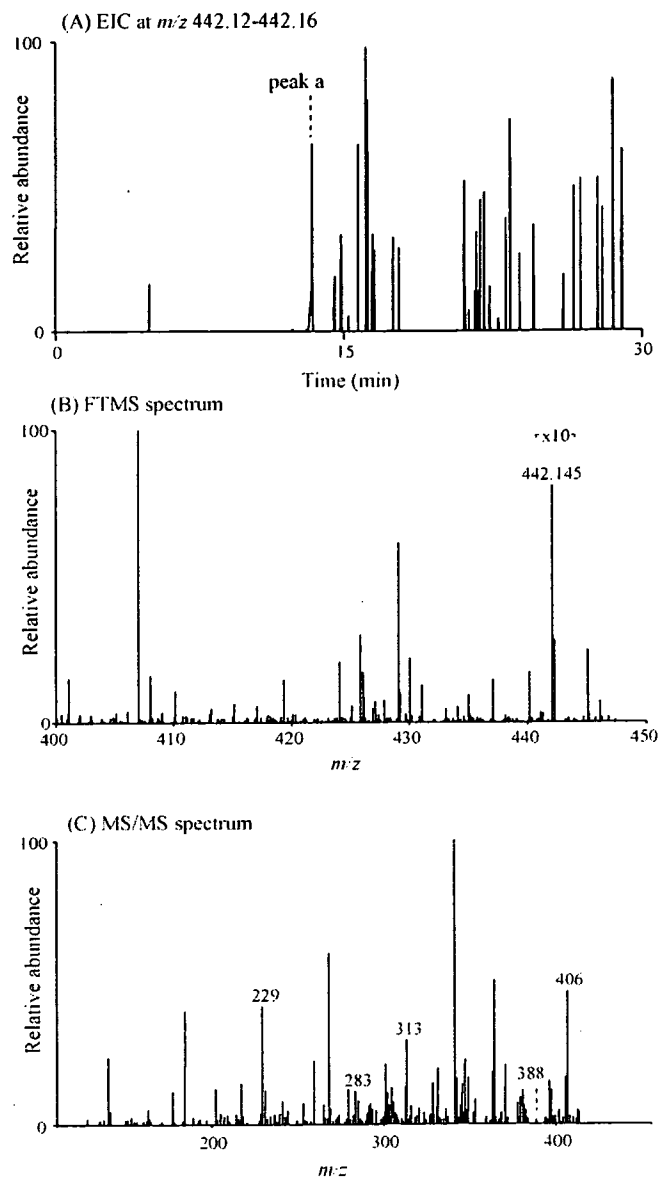

(A) EIC at m/z 442.12-442.16

(B) FTMS spectrum

(C) MS/MS spectrum

Fig. 7. Detection of DMB-NeuGc in the membrane fractions of HL-60RG cells (2.5×10^3) cultured with 10% human serum. (A) EIC at m/z 442.12–442.16 obtained by SIM. (B) Typical MS spectrum of peak a. (C) MS/MS spectrum of [M + H]+ (m/z 442.145) acquired from around peak a.

serum has been reported by Tangvoranuntalul et al. [23], which has raised concerns about NeuGc contamination of cell therapy products through cultivation with human serum. Although using our method, we demonstrated the existence of NeuGc in human cells cultured with human serum, NeuGc could not be detected in human cells cultured in serum-free medium in which no NeuGc exists. These results suggest the difficulty of avoiding NeuGc contamination of cell therapy products during the manufacturing process. Further study to assess the immunogenicity of incorporated NeuGc is necessary to ensure the safety and efficacy of cell therapy products, and our method is useful for the sensitive and quantitative analysis of NeuGc in cell therapy products.

Acknowledgements

References

[1] C. Traving, R. Schauer, Cell Mol. Life Sci. 54 (1998) 1330.

[2] T. Angata, A. Varki, Chem. Rev. 102 (2002) 439.

[3] A. Varki, Glycobiology 2 (1992) 25.

[4] R. Schauer, Adv. Carbohydr. Chem. Biochem. 40 (1982) 131.

[5] S. Kitazume, K. Kitajima, S. Inoue, S.M. Haslam, H.R. Morris, A. Dell, W.J. Lennarz, Y. Inoue, J. Biol. Chem. 271 (1996) 6694.

[6] R. Schauer, J. Haverkamp, M. Wember, J.P. Kamerling, J.F. Vliegenthart, Eur. J. Biochem. 62 (1976) 237.

[7] N. Kawasaki, S. Itoh, M. Ohta, T. Hayakawa, Anal. Biochem. 316 (2003) 15.

[8] M. Nakano, K. Kakehi, M.H. Tsai, Y.C. Lee, Glycobiology 14 (2004) 431.

[9] E.A. Muchmore, S. Diaz, A. Varki, Am. J. Phys. Anthropol. 107 (1998) 187.

[10] A. Irie, S. Koyama, Y. Kozutsumi, T. Kawasaki, A. Suzuki, J. Biol. Chem. 273 (1998) 15866.

[11] H.H. Chou, H. Takematsu, S. Diaz, J. Iber, E. Nickerson, K.L. Wright, E.A. Muchmore, D.L. Nelson, S.T. Warren, A. Varki, Proc. Natl. Acad. Sci. U. S. A. 95 (1998) 11751.

[12] H. Higashi, M. Naiki, S. Matuo, K. Okouchi, Biochem. Biophys. Res. Commun. 79 (1977) 388.

[13] J.M. Merrick, K. Zadarlik, F. Milgrom, Int. Arch. Allergy Appl. Immunol. 57 (1978) 477.

[14] M.J. Martin, A. Muotri, F. Gage, A. Varki, Nat. Med. 11 (2005) 228.

[15] A. Heiskanen, T. Satomaa, S. Tiitinen, A. Laitinen, S. Mannelin, U. Impola, M. Mikkola, C. Olsson, H. Miller-Podraza, M. Blomqvist, A. Olonen, H. Salo, P. Lehenkari, T. Tuuri, T. Otonkoski, J. Natunen, J. Saarinen, J. Laine, Stem Cells 25 (2007) 197.

[16] A.E. Manzi, S. Diaz, A. Varki, Anal. Biochem. 188 (1990) 20.

[17] S. Hara, M. Yamaguchi, Y. Takemori, K. Furuhata, H. Ogura, M. Nakamura, Anal. Biochem. 179 (1989) 162.

[18] M. Bardor, D.H. Nguyen, S. Diaz, A. Varki, J. Biol. Chem. 280 (2005) 4228.

[19] M. Ito, K. Ikeda, Y. Suzuki, K. Tanaka, M. Saito, Anal. Biochem. 300 (2002) 260.

[20] F.N. Lamari, N.K. Karamanos, J. Chromatogr. B 781 (2002) 3.

[21] A. Klein, S. Diaz, I. Ferreira, G. Lamblin, P. Roussel, A.E. Manzi, Glycobiology 7 (1997) 421.

[22] H.H. Chou, T. Hayakawa, S. Diaz, M. Krings, E. Indriati, M. Leakey, S. Paabo, Y. Satta, N. Takahata, A. Varki, Proc. Natl. Acad. Sci. U. S. A. 99 (2002) 11736.

[23] P. Tangvoranuntakul, P. Gagneux, S. Diaz, M. Bardor, N. Varki, A. Varki, E. Muchmore, Proc. Natl. Acad. Sci. U. S. A. 100 (2003) 12045.

Regulatory Aspects of Oncolytic Virus Products

Teruhide Yamaguchi[1,*] and Eriko Uchida[2]

[1]*Division of Biological Chemistry and Biologicals, The National Institute of Health Sciences, Kamiyoga 1-18-1, Setagaya, Tokyo, 158-8501, Japan;* [2]*Division of Cellular and Gene Therapy Products, The National Institute of Health Sciences, Kamiyoga 1-18-1, Setagaya, Tokyo, 158-8501, Japan*

Abstract: Many types of oncolytic viruses, wild-type virus, attenuated viruses and genetically-modified viruses, have been developed as an innovative cancer therapy. The strategies, nature, and technologies of oncolytic virus products are different from the conventional gene therapy products or cancer therapy products. From the regulatory aspects to ensure the safety, efficacy and quality of oncolytic viruses, there are several major points during the development, manufacturing, characterization, non-clinical study and clinical study of oncolytic viruses. The major issues include 1) virus design (wild-type, attenuated, and genetically engineered strains), 2) poof of concept in development of oncolytic virus products, 3) selectivity of oncolytic virus replication and targeting to cancer cells, 4) relevant animal models in non-clinical studies, 5) clinical safety, 6) evaluation of virus shedding. Until now, the accumulation of the information about oncolytic viruses is not enough, it may require the unique approach to ensure the safety and the development of new technology to characterize oncolytic viruses.

Keywords: Gene therapy, cancer therapy, replicating virus.

INTRODUCTION

Oncolytic virus therapy has been developed as a new wave of cancer therapies. These therapies are dependent on the replication-selective nature of these viruses in tumor cells, which provides the marked breaths of cancer therapy. More than one century ago, evidence of oncolytic activity caused by replicating viruses was reported, and it was known the viruses could induce tumor lysis. Using these studies as a point of departure, rare but dramatic responses in cancer patients recovering from viral infections were reported. In the early development of oncolytic virus therapy, wild-type viruses with low pathogenicity to normal tissues, or attenuated viruses were selected for the treatment of cancer patients. However, some adverse events, such as the development of encephalitis in immune compromised patients, were reported [1-3]. Other works reported the oncolytic activity of wild-type or attenuated oncolytic viruses to be transient or limited to the site of injection [4-8]. Recently, attention has focused on overcoming the disadvantages of wild-type or attenuated oncolytic virus therapy, and many genetically modified viruses have been developed for cancer treatment. Progress in the development of genetically engineered oncolytic viruses has been based on recent advances in our understanding of the molecular biology of cancer and viruses, and on advances in genetic engineering technologies of virus genomes. Although many gene therapy clinical studies for the treatment of cancer have been conducted during the past decade using replication-incompetent virus vectors, these studies have not achieved satisfying results. Tumor-selective replicating viruses have been suggested to have an advantage over conventional gene therapy vectors for cancer therapy, and oncolytic viruses, especially genetically modified viruses, must be considered to be a special type of gene therapy product since their principle is directly associated with the transfer of the viral genome as the therapeutic gene [9]. In the present report, we review the development of oncolytic viruses as gene therapy products or attenuated virus products with specific reference to the associated regulatory issues.

Oncolytic virus therapy is based on several strategies, including tumor-selective replication, tumor-selective targeting, and/or the minimization of toxicity to normal cells. Many types of viruses have been utilized in oncolytic virus therapy; including adenovirus, herpes simplex virus (HSV), reovirus, Newcastle disease virus (NDV), vaccinia, measles virus, vesicular stomatitis virus (VSV) and Sendai virus [10-13]. During the development of oncolytic virus products, a number of major issues have arisen with respect to ensuring the quality, safety and efficacy of the products: 1) virus design (wild-type, attenuated and genetically engineered strains); 2) proof of concept in the development of oncolytic virus products; 3) the selectivity of oncolytic virus replication and targeting to cancer cells; 4) relevant animal models in non-clinical studies; 5) clinical safety; and 6) the evaluation of virus shedding. Since the strategies, nature and technologies of oncolytic virus products are different from those of conventional gene therapy products or cancer therapy products, we discuss the regulatory aspects of the development of oncolytic viruses in the present paper.

VIRUS DESIGN AND PRODUCT DEVELOPMENT

While many types of viruses are utilized for oncolytic virus therapies [10, 11, 14], selective replication in tumor cells is essential for the efficacy and safety of oncolytic viruses. Wild-type viruses and naturally occurring attenuated viruses are known to possess the ability to infect and kill transformed cells such as tumor cells. For example, VSV, NDV and reovirus have been used as oncolytic viruses with inherent tumor-selectivity [12, 15-18]. In the case of wild-type viruses or attenuated viruses, the mechanism underlying the virus-selectivity to tumor cells has been analyzed from various points of view. For instance, reovirus has an inherent preference for replicating cells with dysregulated growth factor-signaling cascades by Ras activation [17, 19]. Attenuated strains from HSV-1 have been reported to be potential anti-cancer therapeutics and have necessitated a thorough investigation into the molecular basis of host-cell permissiveness to HSV [20-22]. Since in the

*Address correspondence to this author at the Division of Biological Chemistry and Biologicals, The National Institute of Health Sciences, Kamiyoga 1-18-1, Setagaya, Tokyo, 158-8501, Japan; Tel: +81-3-3700-1926; Fax: +81-3-3707-6950; E-mail: yamaguch@nihs.go.jp